NUMERICAL MODELING FOR STATIC AND DYNAMIC ANALYSIS OF DIELECTRIC ELASTOMER ACTUATORS

A DISSERTATION

Sumitted in partial fulfillment of the requirements for the award of the degree of

Master of Technology

in

Mechanical Engineering

(with specialization in Machine Design Engineering)

by

PANDYA MILIND JAYPRAKASH

DEPARTMENT OF MECHANICAL AND INDUSTRIAL ENGINEERING
INDIAN INSTITUTE OF TECHNOLOGY ROORKEE
ROORKEE - 247667 (INDIA)
MAY,2019

INDIAN INSTITUTE OF TECHNOLOGY ROORKEE

ROORKEE

CANDIDATE'S DECLARATION

I hereby declare that the work carried out in this dissertation entitled, "Numerical modeling for Static and Dynamic analysis of Dielectric Elastomer Actuators" is presented on behalf of partial fulfillment of the requirement for the award of the degree of Master of Technology with specialization in MDE submitted to the department of Mechanical Industrial Engineering, Indian Institute of Technology Roorkee, India, under the supervision and guidance of **Dr. Manish M. Joglekar**, Associate Professor, IIT Roorkee and **Prof. Dr. Bai-Xiang Xu**, TU-Darmstadt.

I have not submitted the matter embodied in this report for the award of any other degree or diploma.

Date: ,2019

Place : Roorkee **(Pandya Milind J.)**

(Er. Number : 17539007)

CERTIFICATION

This is to certify that the above statement made by the candidate is correct to the best of my knowledge and belief.

Dr. Manish M. Joglekar

Associate Professor,

MIED,IIT Roorkee,

Uttarakhand-247667, India

INDIAN INSTITUTE OF TECHNOLOGY ROORKEE

ROORKEE

CANDIDATE'S DECLARATION

I hereby declare that the work carried out in this dissertation entitled, "**Numerical Modeling for Static and Dynamic Analysis of Dielectric Elastomer Actuators**" is presented on behalf of partial fulfillment of the requirement for the award of the degree of **Master of Technology** with specialization in **Machine Design Engineering** and is submitted to Department of Mechanical Industrial Engineering, Indian Institute of Technology Roorkee, India, under the supervision and guidance of Dr. Manish M. Joglekar, Associate Professor, IIT Roorkee and **Prof.** Dr. Bai-Xiang Xu, TU-Darmstadt.

I have not submitted the matter embodied in this report for the award of any other degree or diploma.

Date: 8th May 2019

Place : Roorkee

(Pandya Milind J.)

(Er. Number : 17539007)

CERTIFICATION

This is to certify that the above statement made by the candidate is correct to the best of my knowledge and belief.

Mechanik funktionaler Materialien
Fachbereich 11
Material- und Geowissenschaften
Otto-Berndt-Str. 3
Technische Universität
D-64287 DARMSTADT

8/5/2019

Prof. Dr. Bai-Xiang Xu
Fachgebiet Mechanik funktionaler Materialien
Fachbereich Material- und Geowissenschaften
TU Darmstadt,Germany

Dr. Manish M. Joglekar
Associate Professor,
MIED,IIT Roorkee,
Uttarakhand-247667, India

ACKNOWLEDGEMENT

First of all, I express a profound sense of obligations to the almighty God for showing immense blessing upon me, which made me accomplish this academic task. Words fail to express the noble sacrifice of my parents who brought me to this position.

I would like to express profound gratitude to my guide **Dr. Manish M. Joglekar** , Associate prof., MIED, IIT Roorkee for his invaluable support, encouragement, supervision throughout the work. He has been a great mentor to me and has always led by an example. I would also like to acknowledge **Prof. Dr. Xu** , TU Darmstadt for supervising my work and for her kind guidance. Also, I am grateful to the German Academic Exchange Service (DAAD) for providing a great opportunity to experience the work culture in Germany and for helping me in every way possible throughout my tenure. I would also like to thank Mr. Atul Sharma, Researh Scholar, IIT Roorkee for sharing his knowledge in the field and his constant support. This work could have not been completed without his valuable inputs. I would like to express my gratitude to the teams in both the offices. Their moral support and continuous guidance enabled me to complete my work successfully. Also, I would like to thank my friends and my family, who has always been there for me in though times. Last but not the least, I am thankful and indebted to all those who helped me directly or indirectly in completion of this report.

Abstract

Soft dielectric elastomers are widely employed to build smart devices controlled by electrical potential difference. They find applications in several fields of engineering, ranging from mechanical to biomedical. Most of the work done for the simulation of the behavior of the dielectric elastomer utilize the monolithic formulation for this multiphysics problem, which requires large amount of computational power. This fact significantly limits the ability to simulate complex three dimensional dynamic problems involving complex loading and electromechanical instabilities of DEA. Some recent researches have shown that staggered formulation for the problem can very well reduce the computational time for multiphysics problem and can tackle the electromechanical instabilities very accurately in case of Dielectric Elastomer. In the present study, staggered formulation, in conjunction with the mixed formulation to alleviate the problem of volumetric locking has been presented for the dielectric elastomer. The formulation has been validated by the known theoretical results available in literature. Same formulation has been used to demonstrate behavior of dielectric elastomers under complex loading and boundary conditions. And computational efficiency and accuracy of the proposed formulation has been studied with respect to the monolithic approach.

Contents

List of Figures

Chapter 1

Introduction

1.1 Electroactive Polymers

In today's world, new technologies are trying to mimic the natural organisms as efficiently as possible. In nature, most of the materials are soft materials which can deform in the desired manner. So, Soft materials are getting attention in the research community nowadays. Electroactive polymers(EAP) are soft active materials which can be actuated by electric potential. It can be utilized in the active structures where large deformations are desired, as these electrically active actuators convert electrical energy into mechanical work and can exhibit large strains, in the order of 200% to 300% [Pelrine et al., 2000b]. Also, these materials find their application in many engineering fields such as mechatronics, robotics, bio-medical engineering, medical science, industrial automation, space technologies, etc. [Shankar et al., 2007, Carpi, 2010, Brochu and Pei, 2010]. These applications make them a research interest for comunity.

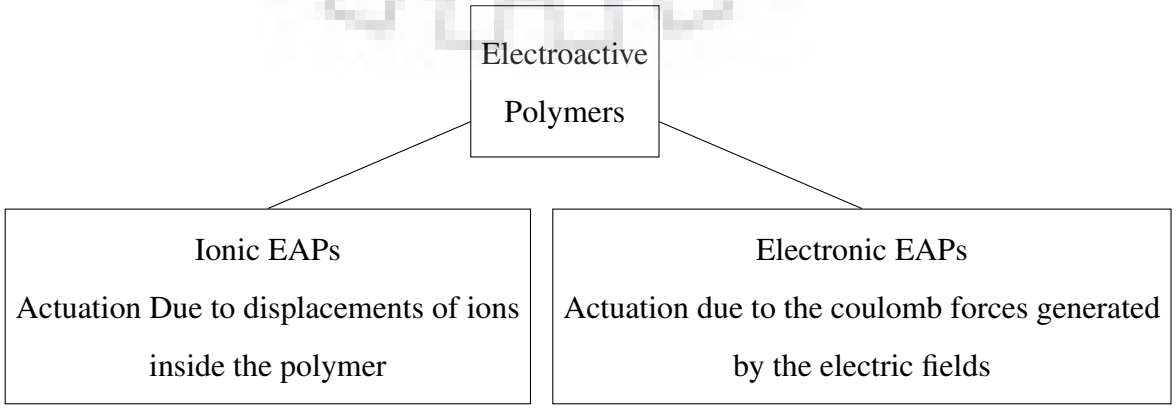

In ionic actuators, electrolyte contains the soluble ions and is filled between two electerodes with low stiffness. When the electric voltage is applied, the mobile cations move towards negatively charged electrodes and take solvent molecules with them as shown in the Fig.1.1.

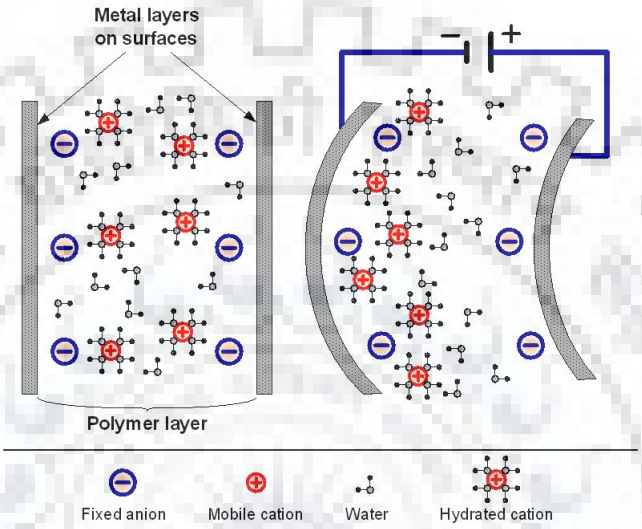

Figure 1.1: Working principle of ionic Electroactive Polymer

Because of this, density towards the negative electrodes increases which results in a swelling of the electrode on the cathode side and shrinking on the anode side. This electrically controlled ion/liquid transfer can cause very fast bending response (upto 100 Hz) [Nam and Kwan, 2012].

1.2 Dielectric Elastomers

Dielectric Elastomers(DEs) are the electronic type electroactive polymers. Electrostatic forces are responsible for their actuation, there is no movement of any ions or molecules during this actuation. Dielectric actuators are very simple in construction and give very fast response. They can be a very good substitute for some rigid body actuators. They are basically an electrically operated soft materials so, they can be utilized to mimic some biological organisms like lenses with variable focal length and muscles. Also, It is very easy to configure them into various structures to achieve complex motion.

Construction and working principle of the dielectric elastomers are shown in the Fig.1.2.

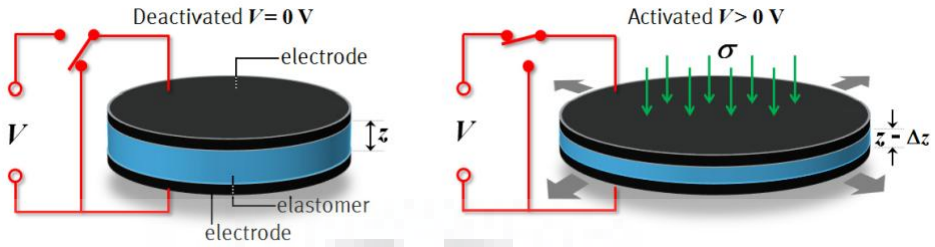

Figure 1.2: Working principle of Dielectric Elastomer [Giousouf and Kovacs, 2013]

It is actually a elastomer sandwiched between two compliant electrodes(very low stiffness value). Graphite powder, caron nanotubes, conductive grease are some of the materials used as the compliant electrodes. For higher performances, liquid metals like GaInSn alloy are also proposed as the compliant electrodes. This electrodes have higher reliability as conductor compared to carbon electrodes mentioned earlier and they maintain there liquid state for very high temperature i.e. 283.5 K to 1573 K. Also, GaInSn has very high electrical conductivity ($\approx 3.1 \times 10^6 Sm^{-1}$), this helps to improve overall performance efficiency of the actuator. Carpi et al.[Carpi et al., 2003] have presented a comparative study for different electrodes. The presented data allows one to select optimum electrode material for the intended purpose like higher stress,strain or efficiency.

The polymer film used as the dielectric elastomer should possess properties like very low stiffness, high dielectric constant and high electrical breakdown strength. The thickness of the films used is 10 to 200μm. Dielectric films can be composed of materials like Dow Corning HS3 Silicone, 3M VHB 4905, 4910 acrylic adhesive and Dow Corning HS3 silicone [Giousouf and Kovacs, 2013, Pelrine et al., 2000b, Carpi, 2010].

Now, when the voltage is applied across the electrodes, the opposite charges on the electrode experiences attractive electrostatic force and squeeze the elastomer in between. This force reduces the thickness of elastomer and elastomer elongates in two in-plane directions. The pressure experienced by the elastomer is known as the Maxwell Pressure and it is directly proportional to square of the applied electric field. The stresses and strains in the film depend on the mechanical and electrical properties of the film and it can be utilized by arranging films in different structures like stacked actuator, tube actuator, bending actuators.

Electric EAPs are very useful in rootics application as they can maintain the induced deformation if actuated under direct voltage supply and can be operated in dry environment. They also have high mechanical energy density. However, activation voltages required for the dielectric elastomer are very high ($>$10 V/μm) and those are close to the breakdown level[Bar-Cohen et al., 2007]. On the contrary, ionic EAPs require only 1-2 volts for actuation. But, most of them require wet medium for actuation. Ionic polymers also have a low electromechanical coupling. They are however ideal for bio-mimetic devices[Bar-Cohen et al., 1999]. In the next section, various instabilities related to Dielectric elastomers have been discussed which limits the performance of the actuators.

1.3 Failure Modes

1.3.1 Electrical Failure

This failure is experienced when the applied electric field crosses a Dielectric strength of the elastomer. Dielectric strength is simply a threshold electrical field value above which the material becomes conductive. One can find the dielectric strength of the DE by plotting experimental breakdown voltage vs total stretch graphs. Factors like temperature, experimental method used, deformation also affect the dielectric strength of DE. It can also be improved by providing pre-streatch before the actuation[Gatti et al., 2014, Tröls et al., 2013].

1.3.2 Instability Failure

It has been reported that the DE actuators (DEAs) are susceptible to a phenomena called pull-in instability when actuated electrostatically. When the stresses imposed due to electrostatic forces inside the elastomer exceeds the elastic forces due to deformation, the elastomer thins out rapidly[Zhao and Sharma, 2017]. This action will further increase the electrical field between the electrodes and this cycle will lead to catastrophic failure of the elastomer film. This limits the maximum deformation that can be produced by DE.

1.3.3 Mechanical Failures

DE actuators are used for the very large deformations but sometimes it reaches the stretching limit of the polymer chain of the material and the elastomer film ruptures. This mechanical failure occurs due to the excessive strain of the polymer.

1.3.4 Surface Instability

Dielectric actuators are basically thin membranes sandwiched between compliant electrodes and thin membranes tend to wrinkle whenever they are subjected to compressive load due to their negligible small bending resistance. Small in-plane compressive stresses can cause membranes to buckle in out of plane direction. This wrinkling can occur in the polymer when the residual stresses in the polymer exceeds a critical value. Wrinkling helps the material to relax by releasing the energy by increasing the surface area. In the most common method to tackle the wrinkling in the structural membranes, bi-axial pre-stress is applied to the membrane materials so they stay in the tensile stress state through out the operation. Additional stretching of the fabric is thus required in order to eliminate potential wrinkles. Dielectric elastomers frequently undergoes voltage induced large deformations. During this deformations, wrinkles can nucleate and propagate through the flat surfaces of the elastomer. But sometimes, these wrinkles are controllable and can also help to get such actuation which are not possible otherwise. In critical optical and space applications, this surface instability can compromise the objective of the mechanism.
One of the major difficuties in simulating the response of DE under electro-mechanical loading is to handle the incompressibility of the elastomer and that imits the ability to predict the actual material behaviour. Also, there has been very few studies which tackles the problem under dynamic conditions. Instailities like wrinkling can only be studied accurately with dynamc formulation for the same. So, we will try to formulate FEM code using MATLAB ® to tackle these difficulties.

1.4 Organization of the Dissertation

The main objective of this work is to present a efficient in-house finite element formulation to simulate dielectric elastomers which can simulate the static and dynamic

response of the DE and predict different kind of instablities prevailing in this multi-physics problem.

- This report is divided into six parts including the chapter of introduction, which gives the idea about new age electroactive polymers and their working principle. An overview of different type of failure modes for the dielectric elastomers has been discussed. Finally, the organization of the report is presented.
- The second chapter gives a brief literature review of the relevant work done in the past and their useful conclusions. Different existing framework for the analysis of the DE has been discussed.
- The Third chapter consists of the theoretical background for the finite element formulation of the problem. Based on these non linear governing equations, a finite element model is presented to study electro-mechanical response of the hyperelastic DEs. It also includes the mathematical hyperelastic material model used for the analysis.
- The fourth chapter presents the energy based lumped parameter analytical analysis for the homogeneous deformation of the DE. These results are used to validate the developed numerical model by comparing both the results for symmetric loading condition.
- After the validation of the developed in-house code, the fifth chapter includes some numerical results obtained using the finite element analysis. The last section concludes the report and discusses some idea which can be pursued in the future.

Chapter 2

Literature Review

Considerable amount of research work has been carried out in the field of DEA since late 90's. In recent times, Many researchers have shown many different types of applications for the dielectric elastomers. Giousouf at el.[Giousouf and Kovacs, 2013] have proposed the use of stacked dielectric elastomers in the pneumatic valve actuation. They have also discussed the desirable properties for elastomers to be used in such applications.

O'Halloran et al.[O'Halloran et al., 2008] has reviewed such applications of dielectric elastomers and has also discussed the technological difficulties in advancement. Use of DEA for the generation of the electricity has been investigated by Pelrine at el.[Pelrine et al., 2001]. This work discusses the basic principle of dielectric elastomer generators and gives an experimental verification. It shows that if small charge is placed on the surface of the elastomer before contraction, then contraction works against the electrostatic field and raises the voltage of the charge. All these application are based on the study of electeromechanical coupling in the dielectric elastomers.

2.1 Electromechanical Coupling

Many efforts have been made to explain the electromechanical coupling effects in dielectric elastomers. Pelrine et al.[Pelrine et al., 1998] has done a pioneer work in this field. They developed the initial model to understand the inner mechanism of the dielectric elastomer. They proposed that the elastic stresses induced in the elastomer due

to the deformation will balance the electrostatic pressure between the electrodes. This electrostatic pressure can be expressed as, $p = \varepsilon_k E^2$,where E is the applied electric field and ε_k is the permittivity of the elastomer material. They have also proposed some actuators based on the EAPs and explored the idea of using DE as smart material. They have used linear elastic material for the explanation but it is not suitable for the large deformation. So, to refine the model further Pelrine et al.[Pelrine et al., 2000a] has studied the effects in nonlinear, high-strain, Mooney–Rivlin model. They have also discussed the highly compliant electrodes and some of the actuator structures incorporating dielectric elastomers.

Goulbourne et al.[Goulbourne et al., 2005] has discussed the non linear dielectric model and potential cardiac pump application. Suo et al.[Suo et al., 2008] has presented a monolithic non-linear theory for the soft dielectric. The nominal stresses and the electric fields are obtained from the free energy density function of the system. This coupled theory can incorporate most of the hyperelastic material models thus giving better insight of the phenomena.

These analytical models are generally limited to simple unconstrained configurations of DEAs involving homogeneous deformations. However, in actual applications, the dielectric elastomers undergo in-homogeneous deformation during the course of actuation. The complex applications of dielectric elastomers such as four finger gripper and high speed tunable lens involve in-homogeneous deformation during their operation. The modeling of dielectric elastomer actuators involving inhomogeneous deformation require sophisticated computational approaches and has been of continued interest.

2.2 Numerical Modeling

O'Brien et al.[O'Brien et al., 2009] has presented a Finite element model to analyze Dielectric elastomer minimum energy structures. They have used membrane element available in FEA package ABAQUS. To use these membrane elements, they have utilized electrostatic energy density in the formulation because directly Maxwell pressure can not be used with the membrane element. So, total energy density is taken as sum of elastic energy due to deformation and electrostatic energy due to electrical field.

This approach was verified with the experimental data. But, authors have noted that this approach can only be used for quasi static problems due to the manner in which it incorporates viscosity.

Wissler and Mazza [Wissler and Mazza, 2007] have used two different approaches for the finite element analysis of the DEA. First approach evaluates the thickness of the DEA under the application of electromechanical pressure on the surfaces (kinetic boundary condition). While in second approach required voltage would be calculated as the function of reduction in the thickness of elastomer(kinematic approach). They concluded that later approach is more efficient as it requires less number of iteration compared to former one.

Qu et al.[Qu and Suo, 2012] have developed a finite element method for dielectric elastomer based on the non-linear field theory of elastomer. Free energy due to stretching of the network and that due to electric field contributes to the total free energy. So, the final effect is superposition of the both loading. So, they have considered two sets of elements sharing same nodes responsible for either stretching or polarization. They have verified the model with analytical data by solving the ODE. This model can be used to analyze some complex actuator designs based on dielectric elastomer. These models does not include viscoelastic effects of the materials under concentration. Viscoelastisity strongly affects the performance of the dielectric elastomer.

Hong et al.[Hong, 2011] presents a finite element model for viscoelastic dielectric. They have studied the dynamic response of the dielectric elastomer and the effects of pre-stress via this model. Park et al.[Park et al., 2012] have presented a three dimensional finite element model for dielectric elastomers. They have captured and analyzed the performance limiting instabilities such as pull in and wrinkling by incorporating inertial effects in the energy formulation.

2.3 Instability analysis

These analytical and finite element models have been used to analyse electromechanical instabilities of the DEA. Also, Li et al.[Li et al., 2013] has studied electromechanical instability for the DE subjected to internal pressure and electrical

loading experimentally. This work also provides paramatric study to harness the maximum work from the higly non linear behaviour of the DE. Joglekar[Joglekar, 2014] has presented an analytic analysis of the instability parameter for DEA with three different material models namely the neo-Hookean, Ogden and Mooney–Rivlin. He has also discussed the effect of material parameters on the dynamic instability parameter.

Zhou et al.[Zhou et al., 2008] have developed a mesh free code to simulate electrically induced deformation of the elastomer. They have studied the nucleation and the propogation of the instability in the elastomer after a critical voltage point is reached via this method. This approach can even be utilized to study more complex loading and boundary conditions.

Thin membranes have been a part of many applications since a long time and they are prone to wrinkle under certain conditions. So, many researchers have focused on the wrinkling of the membrane structures[Roddeman et al., 1987]. Thin membranes wrinkle whenever they are subjected to compressive load due to their negligible small bending resistance. They buckle out-of-plane under the action of even small in-plane compressive stress.This wrinkling can occur in the polymer when the residual stresses in the polymer exceeds a critical value. Wrinkling helps the material to relax by releasing the energy(increasing the surface area). Most common method to remove wrinkles is to apply bi-axial tensile stress to the membrane. Sometimes, to provide some extra tension to the membrane, they are cut to smaller sizes than required [Zheng, 2009].

Dielectric elastomers frequently undergoes voltage induced large deformations. During this deformations wrinkles can nucleate and propagates through the flat surfaces of the elastomer[Mao et al., 2015]. Mao et al.[Mao et al., 2015] has investigated wrinkling in the inflated DE balloon both experimentally and analytically. They reported the effect of voltage on the wrinkling pattern. But it is not necessary that wrinkles will lead to pull in failure, there can be stable wrinkle formation which can be controlled[Plante and Dubowsky, 2006, Li et al., 2018].

Most of the work has been done for the static analysis of the electro-mechanical response of the dielectric elastomer actuators.Work presented here intend to build an in-house code that can analyze the response of the DE under electro-mechanical loading under static and dynamic conditions and can capture instabilities arising in the elastomer due to this loading.

Chapter 3

Non-Linear field theory for Dielectric elastomers

3.1 Governing Equations

This section will covers the non-linear field theory of the dielectric elastomer based on the electromechanical theory introduced by Suo et al.[Suo et al., 2008]. Fig.3.1 shows an arbitrary three dimensional body under electro-mechanical loading, where the body occupies volume Ω enclosed by surface A. The reference coordinate (undeformed configuration) is denoted by X and the deformed coordinates are x. In the reference state, B and T are body force per unit volume and traction force on the surface A respectively. While Q is the charge per unit volume of the body and ω is the charge per unit surface area. This electromechanical loading induces deformation u and electric potential ϕ at the particle in the reference configuration.

The kinematics of the dielectric elastomer can be described in the form of deformation gradient (F) and electric field (E);

$$F_{ij} = \frac{\partial x_i(\mathbf{X}, t)}{\partial X_J} = \frac{\partial u_i}{\partial X_J} + \delta_{ij} \tag{3.1}$$

and

$$\tilde{E}_l = -\frac{\partial \phi(\mathbf{X}, t)}{\partial X_I} \tag{3.2}$$

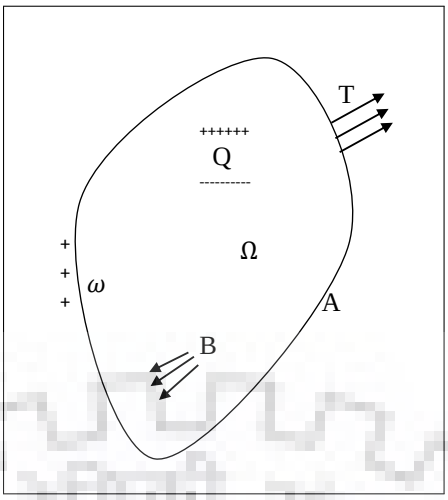

Figure 3.1: Dielectric body under effect of electromechanical loading

To fully describe the electro-mechanical response of the elastomer, constitutive relationships are required. These will provide the relation between (1) electric displacement (D_I) and electric field (E_I), and (2)first Piola-Kirchoff stress (P_{iJ}) and deformation gradient (F_{iJ}). For this, strain energy per unit volume has been defined as Ψ so the total energy would be,

$$W_{int} = \int_{\Omega} \Psi(F_{iJ}, \tilde{E}_J, J) d\Omega \tag{3.3}$$

Assuming the iso-thermal process, the energy balance from the second law of thermodynamics can be written as,

$$\dot{\Psi} - P_{iJ}\dot{F}_{iJ} - D_J\dot{E}_J = 0 \tag{3.4}$$

Free energy density depends on deformation gradient and electric field so, rate of the energy density can be defined as,

$$\dot{\Psi} = \frac{\partial \Psi\left(F_{iJ}, E_J\right)}{\partial F_{iJ}} \dot{F}_{iJ} + \frac{\partial \psi\left(F_{iJ}, E_J\right)}{\partial E_J} \dot{E}_J \tag{3.5}$$

Using this equation we can get the constitutive relations as follows,

$$P_{iJ} = \frac{\partial \Psi\left(F_{iJ}, E_J\right)}{\partial F_{iJ}}, \quad \text{and} \quad D_J = -\frac{\partial \Psi\left(F_{iJ}, E_J\right)}{\partial E_J} \tag{3.6}$$

Now, these elastomers are incompressible materials having poisson's ratio nearly equal to 0.49. This fact adds too many constraints in the discretized finite element problem. This leads to the numerical difficulty known as volumetric locking and it gives overly stiff behavior of the material. There are some numerical methods to overcome this difficulty i.e. F-bar method, reduced integration, B-bar method, hybrid elements [Vossen et al., 2008]. B-bar method in the conjuction with the mixed formulation gives good results[Hughes, 2012]. We have used this strategy for the formulation.

3.2 Q1P0 Formulation

For mixed formulation, four-field variational principle is used which incorporates the displacement field u, electric potential field ϕ, and two additional independent variables which are used to impose the incompressibility constraint in dielectric elastomers, kinematic variable θ which serves as a constraint on the dilational deformation J enforced by the Lagrange multiplier p[Liu et al., 2017].
To apply this principle following definitions are applied;

$$\overline{\mathbf{F}} = \theta^{1/3}\hat{\mathbf{F}}, \quad \hat{\mathbf{F}} = J^{-1/3}\mathbf{F}$$

Where,F is deformation gradient and θ is new kinematic variable. So, the new Cauchy Green tensor can be defined as following,

$$\hat{\mathrm{C}} = \hat{\mathrm{F}}^T\hat{\mathrm{F}} = J^{-2/3}\mathrm{C}$$

So, the internal energy density will be converted in the form of new Cauchy Green tensor,

$$\Psi = \overline{\Psi}\left(\theta^{2/3}\hat{\mathrm{C}}, \widetilde{\mathrm{E}}\right)$$

and the corresponding stress can be defined as,

$$\overline{\mathrm{S}} = \left.\frac{\partial\overline{\Psi}(\mathrm{C}, \widetilde{\mathrm{E}})}{\partial \mathrm{C}}\right|_{\mathrm{C}=\Theta^{2/3}\hat{\mathrm{C}}}$$

Note that, this will affect the mechanical energy part of the equation only. Electrical energy density will be unaffected. Now, the total energy functional can be represented as,

$$\Psi(F_{iJ}, \tilde{E}_J, J) = \Psi^{dev}(u, \theta) + \Psi^{vol}(\theta) + \Psi^{ele}(u, \phi, J) + p(J - \theta) \tag{3.7}$$

Due to the small perturbation in the field variables, change in internal energy can be written as,

$$\delta W^{int} = \int_\Omega \left(\frac{\partial \Psi}{\partial F_{iJ}} \delta F_{iJ} + \frac{\partial \Psi}{\partial E_J} \delta E_J + \frac{\partial \Psi}{\partial p} \delta p + \frac{\partial \Psi}{\partial \theta} \delta \theta \right) d\Omega \tag{3.8}$$

Also, the variation of external work due to the perturbation can be shown as,

$$\delta W^{ext} = \int_A T_i \delta u_i dA + \int_\Omega B_i \delta u_i d\Omega - \int_A \omega \delta \phi dA - \int_\Omega Q \delta \phi d\Omega \tag{3.9}$$

The first variation of F_{iJ} and E_J can be written in terms of the independent variables u and ϕ as shown in Eq. (3.1) and (3.2). Now, principle of virtual work $\delta W^{ext} - \delta W^{int} = 0$ can be evoked to get the weak form of the governing equations to formulate finite element model. We will get,

$$\int_\Omega P_{iJ} \frac{\partial \delta u_i}{\partial X_J} d\Omega = \int_A T_i \delta u_i dA + \int_\Omega B_i \delta u_i d\Omega \tag{3.10a}$$

$$\int_\Omega D_I \frac{\partial \delta \phi}{\partial X_J} d\Omega = -\int_A \omega \delta \phi dA - \int_\Omega Q \delta \phi d\Omega \tag{3.10b}$$

$$\int_\Omega \frac{\partial \Psi}{\partial p} \delta p d\Omega = 0 \tag{3.10c}$$

$$\int_\Omega \frac{\partial \Psi}{\partial \theta} \delta \theta d\Omega = 0 \tag{3.10d}$$

B-Bar Method

In the finite element analysis of incomressible materials an over-stiff response has been observed , this effect is called the locking effect and it can be tackled by mixed formulation(discussed above), Selective integration methods, F-Bar and B-Bar methods,etc. B-Bar method in the conjunction with the mixed formulation can give a very good results[Hughes, 2012].

For the general finite element analysis, the stiffness matrix is given by,

$$K^e = \int_\Omega B^T D B d\Omega$$

and the elemental internal force can be given by,

$$f^e = \int_\Omega B^T \sigma d\Omega$$

Where D is the elasticity tensor and in the selective integration scheme stress is divided in the Deviatoric and dilatation parts and D matrix is updated according to that. But, for the large deformation in polymers dividing this D matrix is not that straight forward. So, as a alternate method B matrix is divided in the two parts, which is called B-bar method. First of all deviatoric part of the B matrix can be found by, $B^{dev} = B - B^{dil}$.
Now, using this deviatoric part, $\overline{B} = B^{dev} + \overline{B}^{dil}$.
This whole approach can be summarized by the equation for the components of $\overline{B}$ matrix,

$$\overline{B}_i = \frac{\int_{\Omega_i} B_i d\Omega}{\int_\Omega d\Omega}$$

The denominator represents the finite element's volume. The above equations present the B matrix for 3D case.

3.3 Finite Element Formulation

To obtain finite element formulation from the weak forms Eq.(3.10), four field variables can be discretized as shown below;

$$u_i = x_i - X_I = \sum_{a=1}^{n} N_a^u u_{ai} \qquad \phi = \sum_{a=1}^{n} N_a^\phi \phi_a$$

$$p = \sum_{a=1}^{n} N_a^p p_a \qquad \theta = \sum_{a=1}^{n} N_a^\theta \theta_a \tag{3.11}$$

The element is chosen such that the interpolation order for p and θ is an order lower than that for u and ϕ, for the consideration of stability[Liu et al., 2017]. Here same tri-linear interpolation functions has been chosen for both displacements(u) and electric potential (ϕ) while, p and θ are constant over an element. So, $N^u = N^\phi = N$ and $N^p = N^\theta = 1$.

This approximation will give us the residual equations which has to be minimized.

$$R^u = \int \frac{\partial \Psi}{\partial F_{iJ}} \frac{\partial N_a^u}{\partial X_J} d\Omega - \int T_i N_a^u dA - \int B_i N_a^u d\Omega \tag{3.12a}$$

$$R^\phi = -\int \frac{\partial \Psi}{\partial E_J} \frac{\partial N_a^\phi}{\partial X_J} d\Omega + \int \omega N_a^\phi dA + \int Q N_a d\Omega \tag{3.12b}$$

$$R^p = \int \frac{\partial \Psi}{\partial p} N^p d\Omega \tag{3.12c}$$

$$R^\theta = \int \frac{\partial \Psi}{\partial \theta} N^\theta d\Omega \tag{3.12d}$$

These all residuals are the function of state variables and include material non-linearities. The finite elememt method aims to make these residuals equal to zero. So, Newton-Rahpson method can be utilized to linearize the equations;

$$\tilde{R}\left(\tilde{A}\right) = R\left(A\right) + \frac{\partial R}{\partial A}\left(\Delta A\right)$$

Where R(A) represents the residuals depending on the state of variables A, and $\frac{\partial R}{\partial A}$ is called tangent stiffness matrix. So, ΔA should be such that the residuals at the next stage would be zero. So;

$$\left(\Delta A\right) = -\left(\frac{\partial R}{\partial A}\right)^{-1} R\left(A\right)$$

The final linearized equations in the matrix form can be represented as;

$$\begin{bmatrix} \Delta u \\ \Delta \phi \\ \Delta p \\ \Delta \theta \end{bmatrix} = -\begin{bmatrix} k^{uu} & k^{ue} & k^{up} & 0 \\ k^{ue} & k^{ee} & 0 & 0 \\ k^{pu} & 0 & 0 & k^{p\theta} \\ 0 & 0 & k^{\theta p} & k^{\theta\theta} \end{bmatrix}^{-1} \begin{bmatrix} R^u \\ R^\phi \\ R^p \\ R^\theta \end{bmatrix} \tag{3.13}$$

This is a monolithic coupled formulation and can be solved for the increment in the field variables at each step of loading. Here, K^{ij} terms denote the derivatives of the residuals with respect to the variable i and j. The definations of these tangent stiffness matrix

members can be given as;

$$K^{uu} = \int_{\Omega} \frac{\partial^2 \psi}{\partial F_{iJ} \partial F_{kL}} \frac{\partial N_a^u}{\partial X_J} \frac{\partial N_b^u}{\partial X_L} d\Omega \tag{3.14a}$$

$$K^{u\phi} = -\int_{\Omega} \frac{\partial^2 \psi}{\partial F_{iJ} \partial E_L} \frac{\partial N_a^u}{\partial X_J} \frac{\partial N_b^\phi}{\partial X_L} d\Omega, K^{\phi u} = \left[K^{u\phi}\right]^T \tag{3.14b}$$

$$K^{\phi\phi} = \int_{\Omega} \frac{\partial^2 \psi}{\partial E_J \partial E_L} \frac{\partial N_a^\phi}{\partial X_J} \frac{\partial N_b^\phi}{\partial X_L} d\Omega \tag{3.14c}$$

$$K^{up} = \int_{\Omega} \left(\frac{\partial N^u}{\partial x_j} \delta_{ij} N^p \right) d\Omega, K^{pu} = [K^{up}]^T \tag{3.14d}$$

$$K^{p\theta} = -\int_{\Omega} N^p N^\theta d\Omega, K^{\theta p} = \left[K^{p\theta}\right] \tag{3.14e}$$

$$K^{\theta\theta} = \int_{\Omega} N^\theta \frac{d^2 \psi^{vol}}{d\theta d\theta} N^\theta d\Omega \tag{3.14f}$$

So, these tangent matrices depend on the energy functional of the material. After getting these linearized equations,we can solve them for increment in the field variables and they can be updated after each iteration as $A^{n+1} = A^n + \Delta A$.The algorithm for the monolithic solution is given in Fig.3.2.

Staggered Formulation

As discussed in the previous section, multiphysics problems can be solved by monolithic approach with good accuracy but it requires large amount of computational power as the complexity of the problem increases. Also, it is hard to compute the stiffness matrices for individual field and computing every degree of freedom at once increases the simulation cost[Seifi and Park, 2016]. So the staggered explicit-implicit algorithm can be used to solve these multiphysics problems. In this algorithm the structural dynamic problem is solved separately first and with the use of the solution of structural degree of freedom, electrical problem is solved implicitly. This method also provides the flexibility to choose how the structural problem would be solved either explicitly or implicitly. Here, momentum equations are solved by implicit predictor-corrector method as it gives the stable results. Momentum equation for the dynamic structural part can be written as,

$$\mathbf{Ma} = f_m^{ext} - f_m^{int} = f_m$$

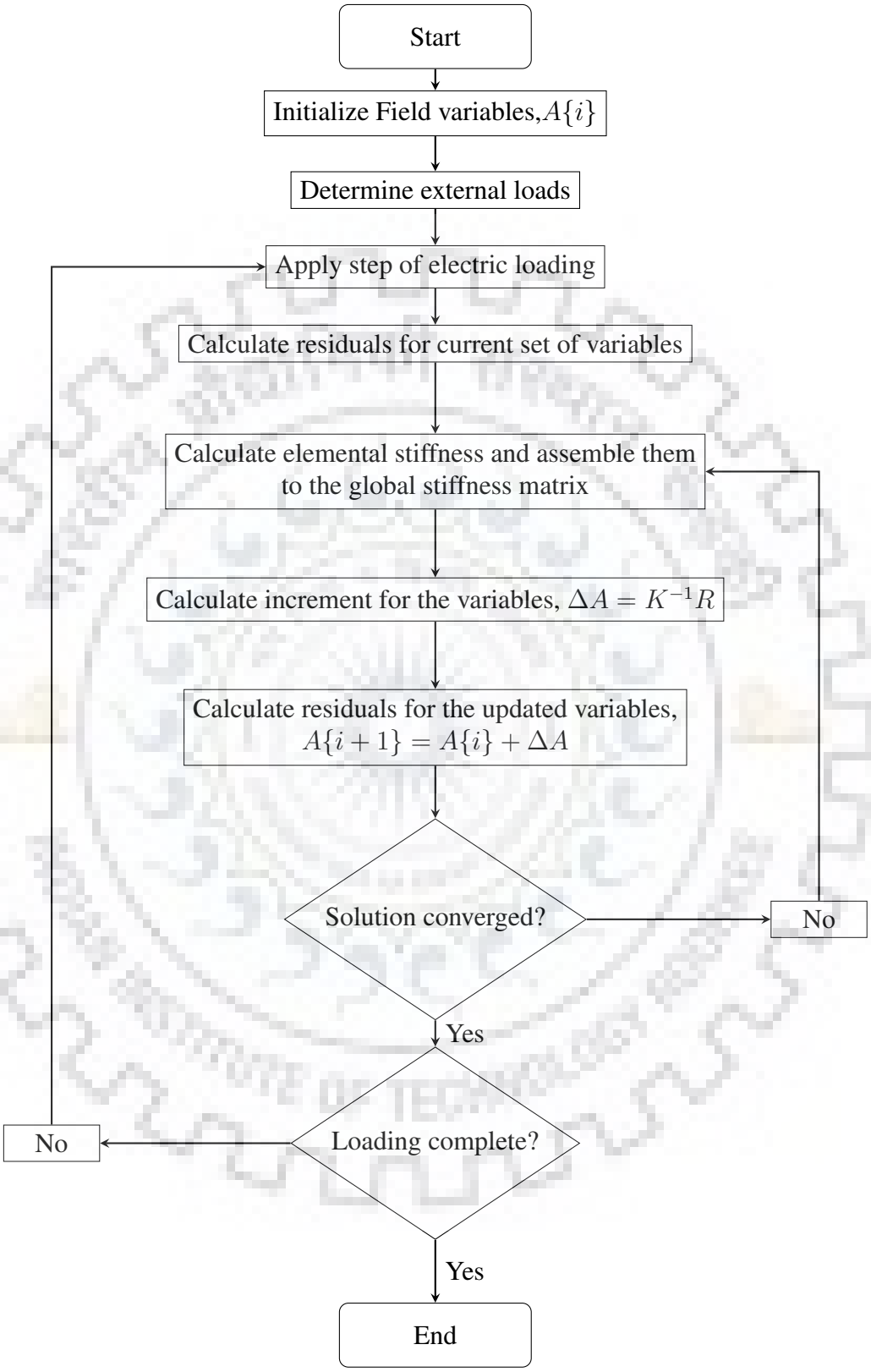

Figure 3.2: Flowchart for Monolithic formulation

Where discretized internal and external forces can be given as,

$$\mathbf{f}_m^{ext} = \int_\Omega B_i N^A d\Omega + \int_A T_i N^A dA$$
$$\mathbf{f}_m^{int} = \int \overline{P}_{iJ} \frac{\partial N^A}{\partial X_J} d\Omega \tag{3.15a}$$

Now if the state of variables from the previous step is (u_n, v_n, a_n), then the predicted values of structural degrees of freedom can be written as following,

$$\mathbf{u}_{pr} = u_n + \Delta t v_n + \Delta t^2 \left(\frac{1}{2} - \beta\right) a_n \tag{3.16a}$$

$$\mathbf{v}_{pr} = v_n + \Delta t \left(1 - \gamma\right) a_n \tag{3.16b}$$

Now, the residual for the displacement field can be given as,

$$\mathbf{R}^u = \mathbf{f}_m^{ext} - \mathbf{f}_m^{int} - \mathbf{Ma} \tag{3.17}$$

Now the required increment in the acceleration can be found such that this residual reduces to zero,

$$\Delta \mathbf{a} = \mathbf{M}^{-1} \mathbf{R}^u$$

So, acceleration can be updated as $\mathbf{a}_{n+1} = \mathbf{a}_n + \Delta \mathbf{a}$. Now, the corrected values of the displacement and velocity can be found out,

$$\mathbf{u}_{n+1} = \mathbf{u}_{pr} + \Delta t^2 \beta \mathbf{a}_{n+1} \tag{3.18a}$$

$$\mathbf{v}_{n+1} = \mathbf{v}_{pr} + \Delta t \gamma \mathbf{a}_{n+1} \tag{3.18b}$$

Now, these values can be used to solve electrostatic equation of the problem. The algorithm for the same is shown in the Fig.3.3. In both of the algorithm discussed above, the euclidean norm of the residual vectors has been used as the convergence criteria. The tolerance limit for the norm is taken as 10^{-8} for all the numerical simulations in the report. In the next section, Neo-Hookean material model has been discussed.

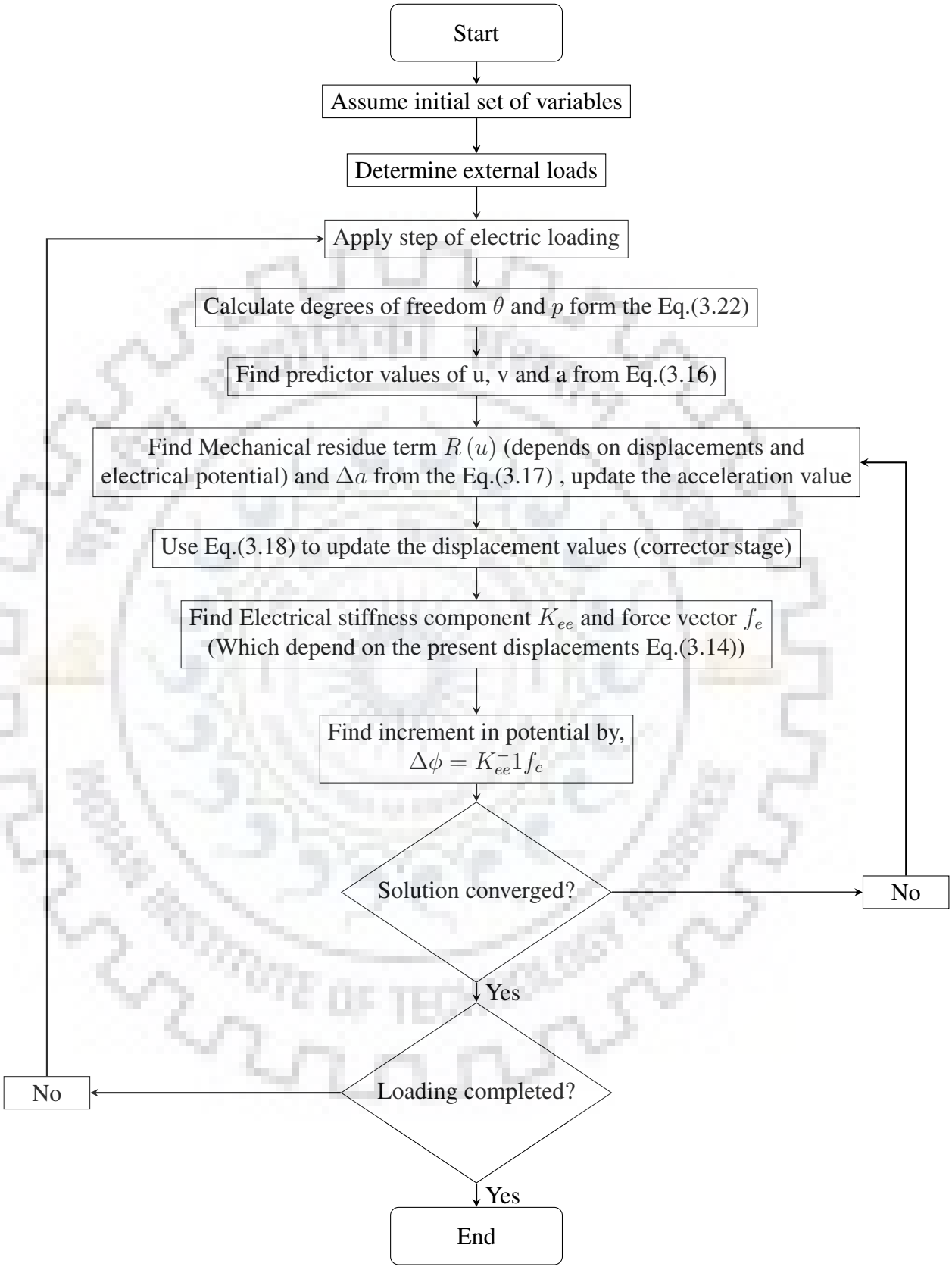

Figure 3.3: Flowchart for Staggered formulation

3.4 Material Model

To model the dielectric elastomer , total strain energy of the system is considered as summation of mechanical and the electrical parts. In present study, ideal dielectric elastomer has been considered which implies that there is no inertial or frictional loss in the system. And to employ the mixed formulation a langrange multiplier term has to be added. So, the final energy density function can be written as following,

$$\Psi(F_{iJ}, \tilde{E}_J, J) = \Psi^{dev}(u, \theta) + \Psi^{vol}(\theta) + \Psi^{ele}(u, \phi, J) + p(J - \theta) \tag{3.19}$$

Where,

Ψ^{dev} is the deviatoric part and Ψ^{vol} is the volumetric part of the mechanical energy due to deformation

Ψ^{ele} is the electrical free energy due to potential difference

To accommodate the large deformation, Neo hookean hyperelastic material model has been used. So, the total energy functional can be written as,

$$\Psi = \underbrace{\frac{G}{2}\left[J^{-2/3}C_{kk} - 3\right]}_{Dev} + \underbrace{\frac{K}{2}(\ln\theta)^2}_{Vol} - \underbrace{\frac{\varepsilon}{2}JC_{pq}{}^{-1}E_pE_q}_{Ele} + p(J - \theta) \tag{3.20}$$

Where,

C_{kk} gives the first invariant of the cauchy-green deformation tensor,

J represents the determinant of the deformation gradient while E is the applied electric field,

G, K, and ε are shear modulus , bulk modulus and the permitivitty of the material respectively.

The electric displacement in the activated region can be given as,

$$D_I = -\frac{\partial\Psi}{\partial E_I} = \varepsilon J E_K C^{-1}_{KI},$$

And the nominal stress is,

$$\begin{aligned} P_{iJ} &= \frac{\partial\Psi}{\partial F_{iJ}} = 2F_{iM}\frac{\partial\Psi}{\partial C_{JM}} \\ &= F_{iM}[GJ^{-2/3}\{\delta_{JM} - \frac{1}{3}C_{KK}C^{-1}_{JM}\} + \varepsilon J E_p E_Q\{C^{-1}_{pM}C^{-1}_{Jq} - \frac{1}{2}C^{-1}_{JM}C^{-1}_{pq}\}] \end{aligned} \tag{3.21a}$$

The residuals for the variables p and θ can be written from Eq.(3.12) as following,

$$R^p = \int_\Omega \{J - \theta\}\, d\Omega \tag{3.22a}$$

$$R^\theta = \int_\Omega \left\{ k \times \frac{\ln \theta}{\theta} \right\} d\Omega \tag{3.22b}$$

These residuals are linear in nature and can be solved directly by comparing them to zero. This will be useful for the staggered formulation used for dynamic analysis. The stiffness matrix component for this material can be obtained using Eq.(3.14).The second order differentiation of the energy term used in stiffness matrix are listed below,

$$\frac{\partial^2 \psi}{\partial E_J \partial E_L} = -\varepsilon J C^{-1}_{JL} \tag{3.23}$$

$$\begin{aligned}
&\frac{\partial^2 \Psi}{\partial F_{iJ} \partial F_{kL}} = \frac{\partial P_{iJ}}{\partial F_{kL}} \\
&= \delta_{ik} G J^{-2/3} \left(\delta_{JM} - \tfrac{1}{3} C_{KK} C^{-1}_{JM}\right) + \varepsilon J E_I E_K \delta_{ik} \left(C^{-1}_{KJ} C^{-1}_{IL} - \tfrac{1}{2} C^{-1}_{JL} C^{-1}_{KI}\right) \\
&+ \tfrac{2G}{3} J^{-2/3} F_{iM} F_{kN} \left[\tfrac{C_{KK}}{2} \left(C^{-1}_{JL} C^{-1}_{MN} + C^{-1}_{JN} C^{-1}_{Ml}\right) - C^{-1}_{JM} \delta_{LN} - C^{-1}_{LN} \left(\delta_{JM} - \tfrac{C_{KK}}{3} C^{-1}_{JM}\right)\right] \\
&+ \tfrac{1}{2} \varepsilon J E_I E_K F_{iM} F_{kN} C^{-1}_{IK} \left(C^{-1}_{JL} C^{-1}_{MN} + C^{-1}_{IK} C^{-1}_{ML}\right) \\
&+ \varepsilon J E_I E_K F_{iM} F_{kN} C^{-1}_{IL} C^{-1}_{NK} C^{-1}_{JM} \\
&+ \varepsilon J E_I E_K F_{iM} F_{kN} C^{-1}_{LN} \left(C^{-1}_{IJ} C^{-1}_{KM} - \tfrac{1}{2} C^{-1}_{IK} C^{-1}_{JM}\right) \\
&- \varepsilon J E_I E_K F_{iM} F_{kN} C^{-1}_{IJ} \left(C^{-1}_{KL} C^{-1}_{MN} + C^{-1}_{KN} C^{-1}_{ML}\right) \\
&- \varepsilon J E_I E_K F_{iM} F_{kN} C^{-1}_{KM} \left(C^{-1}_{IL} C^{-1}_{JN} + C^{-1}_{IN} C^{-1}_{JL}\right)
\end{aligned} \tag{3.24}$$

This finite element formulation is validated in the next chapter by comparing its results with those of analytical lumped parameter analysis. Further, the developed code is used to simulate homogeneous as well as inhomogeneous deformation of the dielectric elastomers under electro-mechanical loading.

Chapter 4

Validation of the Model

4.1 Static and Dynamic instability parameters for Dielectric elastomer

In this section, the above discussed model has been verified by some standard known results. Joglekar [Joglekar, 2014] has proposed a energy based approach to find out the static and dynamic instability parameters using lumped parameter model. The same instability parameters have been calculated by the finite element model proposed in the chapter 3. Fig.4.1 shows the schematic of DEA under a electrostatic loading without any mechanical constraints.

The dielectric film has original dimensions of $2L \times 2L \times 2H$ ad has been sandwiched between two compliant electrodes with negligible stiffness. X_1, X_2 and X_3 are reference coordinates, while x_1, x_2 and x_3 represents the deformed coordinates. The electrostatic force is applied through a time-varying potential difference $V_a(t)$. Because of the applied potential difference along thickness direction, the membrane contracts in its thickness direction and expands in the lateral directions. The reduction in the thickness direction $(X3)$ can be described by defining stretch ratio as $\lambda = h/H$, where h and H are current and reference thickness of the membrane respectively. Now,if the symmetry and incompressibility conditions are applied one can write that,

$$x_1 = \frac{X_1}{\sqrt{\lambda}}, \quad x_2 = \frac{X_2}{\sqrt{\lambda}} \quad and \quad x_3 = \lambda X_3 \tag{4.1}$$

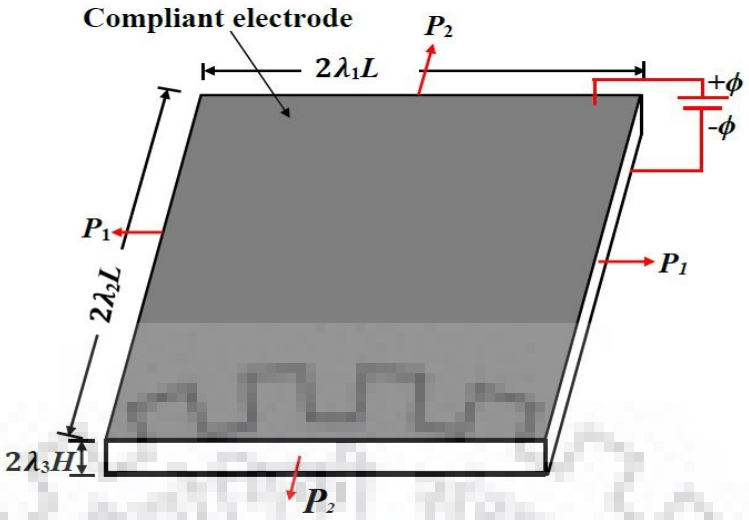

Figure 4.1: Dielecric elastomer under loading

Where λ is stretch in thickness direction.

Now, the total strain energy of the dielectric elastomer can be defined as the sum of both mechanical and the electrical energies in the system, $U = W_m + W_e$.

The strain energy for the Neo- Hookean model per unit volume as a function of the principle stretches can be written as,

$$W_m = \frac{\mu}{2}\left(\lambda_1^2 + \lambda_2^2 + \lambda_3^2 - 3\right) \tag{4.2}$$

Where, μ is the shear modulus,

λ_i is the stretch in corresponding direction.

By applying the fact that , $\lambda_1 = \lambda_2 = 1/\sqrt{\lambda_3} = \lambda$, total strain energy in the deformed state is,

$$W_m = \frac{8HL^2\mu}{2}\left(\frac{2}{\lambda} + \lambda^2 - 3\right) \tag{4.3}$$

The strain energy due to electrostatic force can be written as,

$$W_e = -8HL^2\left(\frac{\varepsilon E_a^2}{2\lambda^2}\right) \tag{4.4}$$

Where, ε is the permittivity and nominal electric field $E_a = \frac{V_a}{2H}$. Now, putting values of Eq.(4.3) and Eq.(4.4) in total strain energy equation and differentiating it with respect to

λ to find the saddle point of the equation, we will get

$$2L^2\frac{\varepsilon V_a^2}{H\lambda^3} = 8HL^2\mu\left(\frac{1}{\lambda^2} - \lambda\right) \tag{4.5}$$

This represents the force balance between electrostatic attraction force and the mechanical restoring force. It shows the relation between applied voltage and stretch for the minimum total strain energy of the system. To find the instability parameter, one has to differentiate Eq.(4.5) with respect to λ , $\frac{dV_a}{d\lambda} = 0$. This gives critical stretch $\lambda_s = 0.630$ and corresponding dimensionless nominal electric field as,

$$e_s = \frac{V_s}{2H}\sqrt{\frac{\varepsilon}{\mu}} = 0.6870 \tag{4.6}$$

This λ_s and e_s are the static instability parameters for the dielectric elastomer.
For the dynamic instability parameters, Joglekar [Joglekar, 2014] has suggested that total electrostatic energy supplied to the system is stored as potential and kinetic energy of the system. At the time of dynamic instability, overshoot in the thickness stretch is maximum and at that point velocity and thus kinetic energy tends to zero. So, total supplied electrostatic energy upto that point is equal to the total strain energy of the system. Now, this total energy upto the dynamic instability can be found out by integrating Eq.(4.5) form $\lambda = 1$ to $\lambda = \tilde{\lambda}$, where $\tilde{\lambda}$ is the stretch ratio upto which energy is to be calculated.

$$\int_1^{\tilde{\lambda}} \frac{2L^2\varepsilon\tilde{V}_{\mathrm{a}}^2}{H\lambda^3}d\lambda = \int_1^{\tilde{\lambda}} 8HL^2\mu\left\{\frac{1}{\lambda^2} - \lambda\right\}d\lambda$$

this can be reduced to,

$$\tilde{V}_{\mathrm{a}}^2 = \frac{4H^2\mu}{\varepsilon}\frac{\left(3\tilde{\lambda}^2 - 2\tilde{\lambda} - \tilde{\lambda}^4\right)}{\left(\tilde{\lambda}^2 - 1\right)} \tag{4.7}$$

Now to arrive at the critical voltage value, we need to apply instability condition that states that any further increment in voltage will result in infinite stretch amplitude so,$\frac{d\tilde{V}_a}{d\tilde{\lambda}} = 0$ This results in,

$$\frac{2}{(\tilde{\lambda}+1)^2} - 2\tilde{\lambda} = 0 \tag{4.8}$$

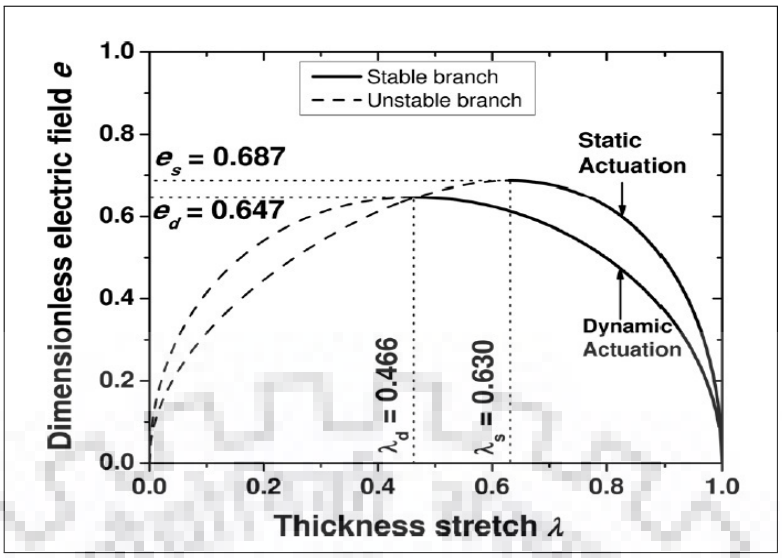

Figure 4.2: Analytical solution for Static and Dynamic instability parameters for Dielectric elastomer[Joglekar, 2014]

By solving this equation we can get the dynamic instability stretch value (λ_d) and using that in the Eq.(4.4) we can find out he minimum voltage required for the dynamic instability of dielectric elastomer.

$$\lambda_{\mathrm{d}} = 0.4656 \qquad\qquad e_{\mathrm{d}} = \frac{V_{\mathrm{d}}}{2H}\sqrt{\frac{\varepsilon}{\mu}} = 0.647$$

Fig.4.2 shows the graph between stretch ratio and dimensionless electric field for the static and dynamic cases. Critical values for the corresponding cases are marked in the figure. Further, Joglekar [Joglekar, 2014], using integration of equation of motion, has reported that response of the DEA for the step voltage less than the critical voltage is periodic and any small increase in the voltage value will result in nonperiodic response from the actuator and actuator will finally break down. Fig.4.3 shows the response of the DEA found analytically for different voltage values.

4.2 Numerical Analysis

This same system has been solved by the finite element formulation with eight noded $U8/E8/P1/J1$ element which has 34 degree of freedom per element. To ensure the incompressibility condition, we have taken the bulk modulus K as five orders of magnitude higher than the shear modulus G, i.e., $K = 10^5 G$. Further, to tackle the issues related to volumetric locking, we have used the B-bar method discussed above.

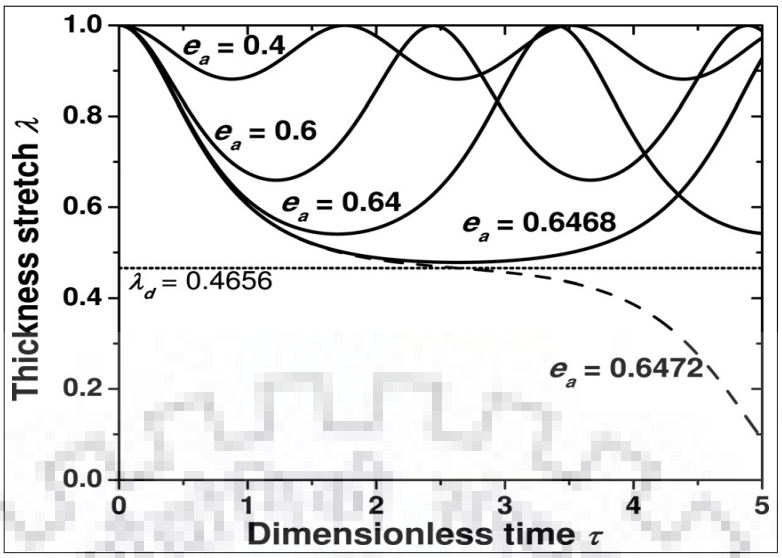

Figure 4.3: Time-history response for DEA under step voltage for different values of the nominal electric field[Joglekar, 2014]

[h!] Fig.4.4 shows the comparison of the static instability parameters calculated by both

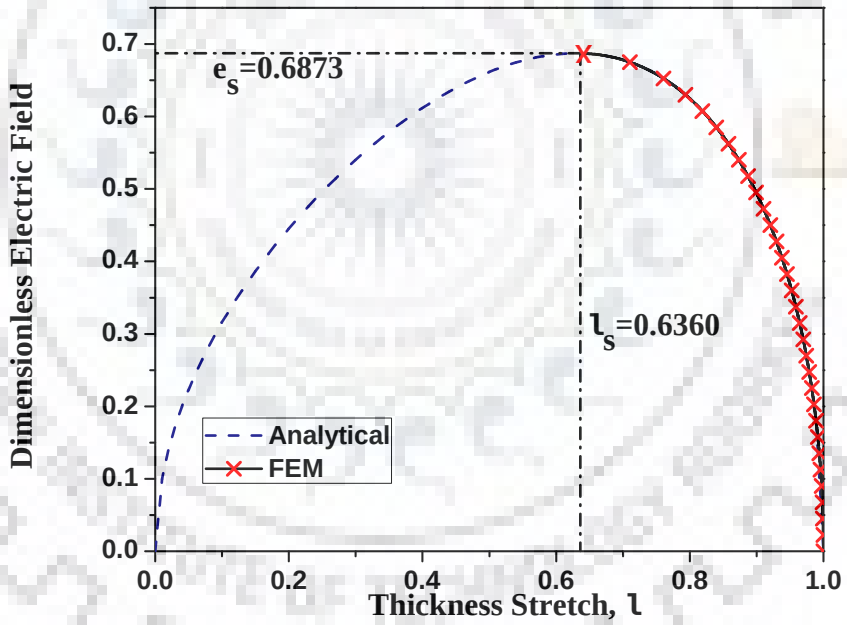

Figure 4.4: Static instability parameters by lumped parameter model and FEM

analytical method discussed above and the finite element formulation. Finite element method gives the static instability parameters as , $\lambda_s = 0.636$ and $e_s = 0.6873$, which are very much in agreement with the theoretically calculated values.

Now, the dynamic response of the DEA for different step voltages are shown in the Fig.4.5. The periodic response can be noticed for the voltages below the critical value $(e_d = 0.6472)$. And for the critical voltage value, the actuator attains stagnation stage at

the critical stretch ratio ($\lambda_d = 0.4656$) and after that becomes instable. These values are very well in agreement with the lumped parameter analysis. Fig.4.6 examines the

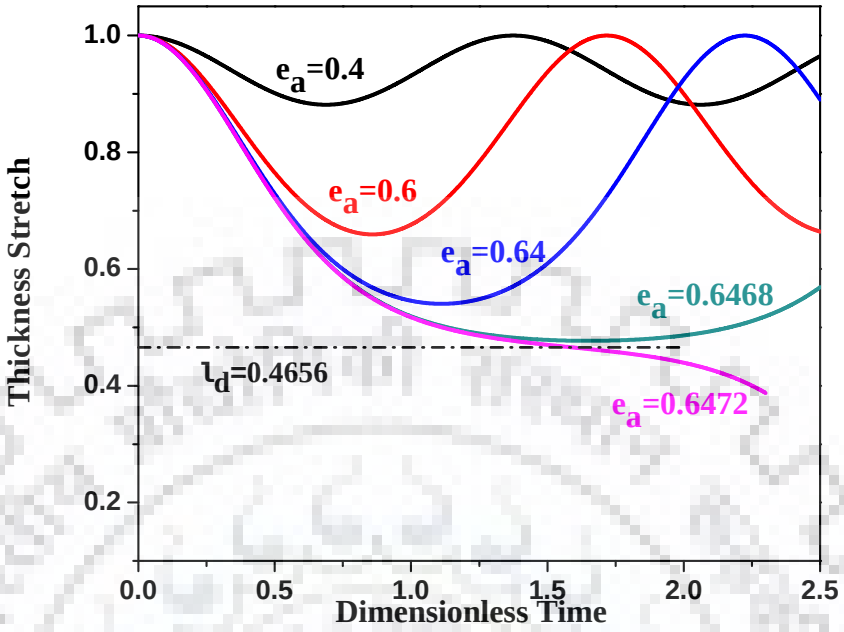

Figure 4.5: Time-history response of the DE under different value of step voltages

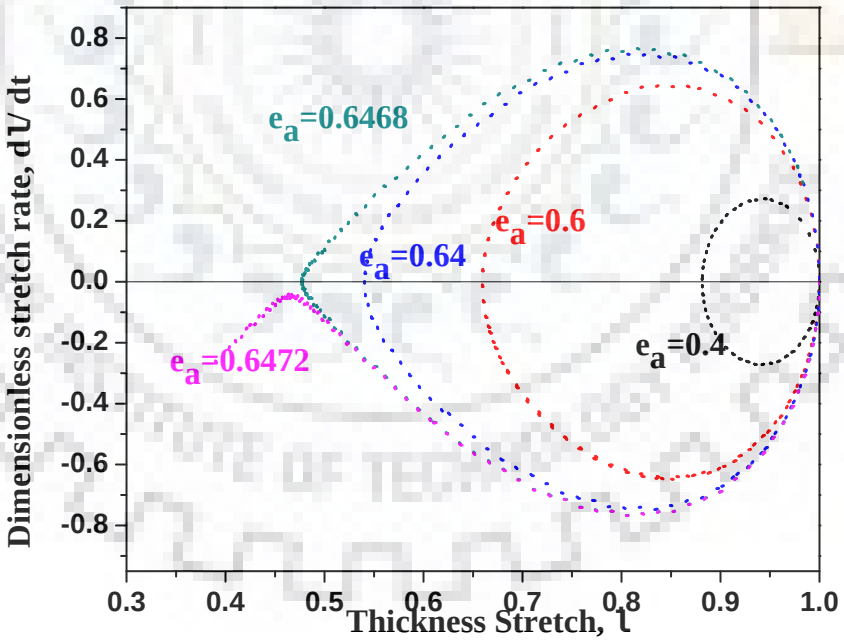

Figure 4.6: Static instability parameters by lumped parameter model and FEM

response of the DEA system on phase plane plot. Voltages below e_d value gives the periodic contours while, at the critical voltage value system reaches stagnation stage at the critical stretch, i.e. $\lambda_d = 0.4656$.

These results confirm that the developed finite element model can analyze the dielectric

elastomer system with fairly good accuracy. So, this model is validated and can be used for different boundary conditions and loading.

Now in the next chapter, we will discuss some static and dynamic numerical results obtained using this model. This will demonstrate the ability of the code to capture the deformation of the actuator under electro-mechanical loading and also the instability in the elastomer.

Chapter 5

Numerical Results

In this chapter, numerical results for dielectric elastomer actuators have been presented based on the formulation discussed in the previous chapters. Examples presented below also includes the electromechanical surface instability in the DEA. This examples show the robustness of the developed code to solve the complex loading and boundary conditions for different DEA structures.

5.1 Effect of prestress on static instability parameters

Prestress given to the DE can improve the performance of the actuator as it allow DE to have higher stretch ratios[Sharma et al., 2017]. Here, We have consider an actuator under symmetric conditions with equal lateral prestress applied.We can write the total potential energy for this system as[Joglekar, 2015],

$$U = \Omega \left[W\left(\lambda_a\right) - \frac{2S}{\sqrt{\lambda_a}} - \frac{\epsilon E_a^2}{2\lambda_a^2} \right] \tag{5.1}$$

Where, $W\left(\lambda_a\right)$ is the strain energy due to deformation and can be taken from Eq.(4.1) and S is the bi-axial traction applied i.e. $P_1 = P_2 = S$.

For the stationary condition $\frac{dU}{d\lambda_a} = 0$,

$$\frac{e^2}{\lambda_a^3} = -\frac{1}{\mu_1}\frac{dW}{d\lambda_a} - \frac{\Gamma}{\lambda_a\sqrt{\lambda_a}} \tag{5.2}$$

where,$e =$ dimensionless electric field $= E_a\sqrt{\epsilon/\mu_1}$

$\Gamma =$ dimensionless pre-stretch parameter $= S/\mu$

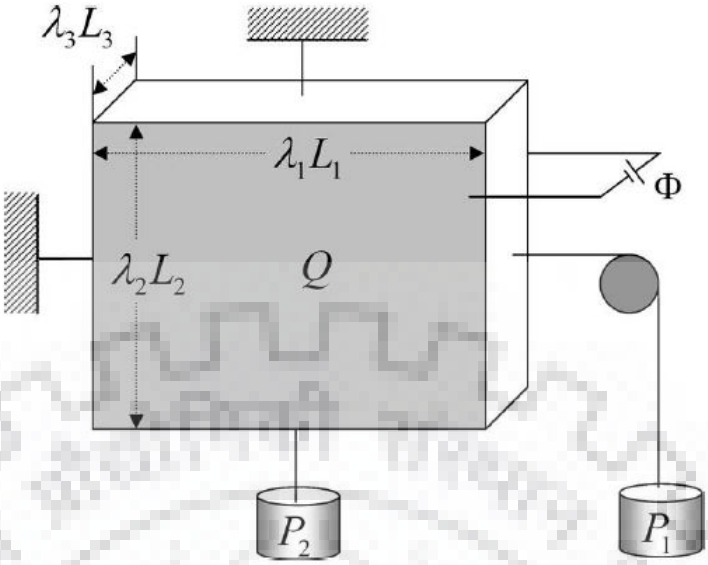

Figure 5.1: Voltage - Thickness stretch graph for $\Gamma = 1$

When we use strain energy function for Neo-Hookean model, we get,

$$e = \left\{\lambda - \lambda^4 - \Gamma\lambda^{3/2}\right\}^{1/2} \tag{5.3}$$

Instable condition can be defined as the point where voltage-stretch graph has zero slope,i.e. $de/d\lambda = 0$. And as we can see, this point now depends on the value of Γ. From the study of same DE, under influence of different stretch ratio, it can be seen that DE can sustain larger thickness stretch with pre-stretch application and instability stretch value increases with increasing pre-stretch.

Now, this effect of prestress is observed using the developed finite element model. To apply prestress, we have applied the mechanical force on the lateral sides as the external force and solved the mechanical force system first. Now, the electrical loading has been applied on this deformed configuration. Fig.5.2 to Fig.5.4 shows the comparison between analytical and numerical results for the prestress value $\Gamma = 1, 1.5$ and 2. The table below shows the instability parameters for all three cases.

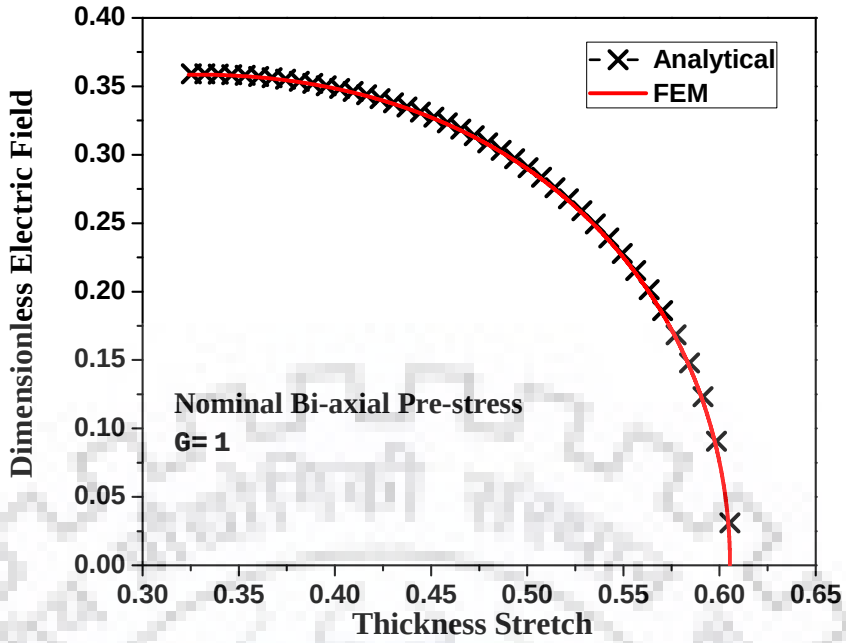

Figure 5.2: Voltage - Thickness stretch graph for $\Gamma = 1$

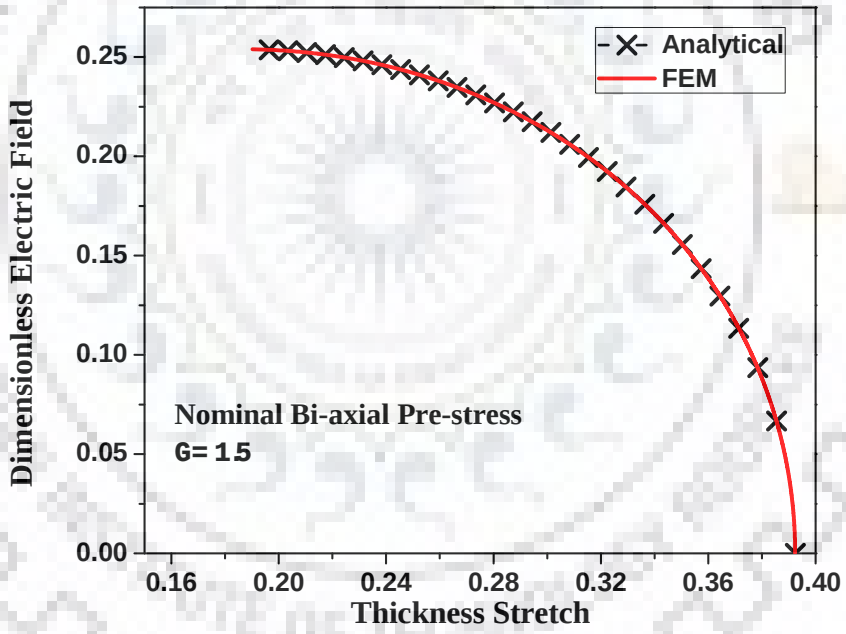

Figure 5.3: Voltage - Thickness stretch graph for $\Gamma = 1.5$

Prestress	$\Gamma = 1$		$\Gamma = 1.5$		$\Gamma = 2$	
	Analytical	FEM	Analytical	FEM	Analytical	FEM
λ_s	0.3279	0.3239	0.1872	0.1902	0.1099	0.1087
e_s	0.3585	0.3587	0.2539	0.2549	0.19206	0.1921

Table 5.1: Static instability parameters for different prestress values

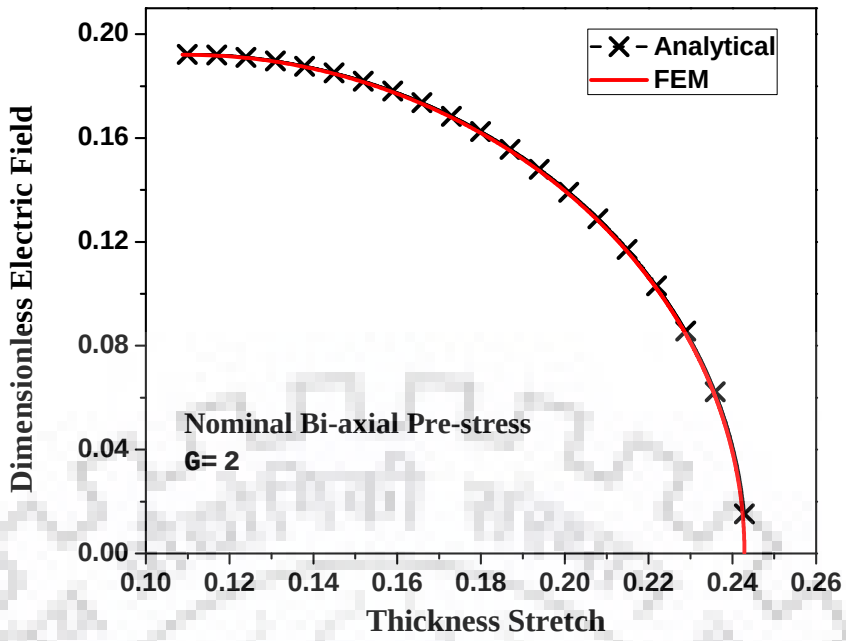

Figure 5.4: Voltage - Thickness stretch graph for $\Gamma = 2$

5.2 Bi-layered Bending Actuator

Here, we have discussed the bi-layered bending actuator made from the dielectric elastomer. Fig.5.5 shows the construction of the bending actuator. It has dimensions of $20cm \times 4cm \times 1cm$. The actuator is isotropic elastomer with same material properties throughout but the upper half is sandwiched between two compliant electrodes and electrical potential ϕ has been applied across it. The active and passive layers of the actuators are perfectly bounded. When actuated, the dielectric elastomer part will shrink in the thickness direction and tries to elongate in the length direction but as it is bonded with the other non-actuated part, this action will trigger the bending of the actuator. Direction $X2$ of the actuator is normal to the page going inward. All the Dirichlet and electrical boundary conditions are listed below,

- Displacement in $X3$ direction is zero on $X3 = 0$ surface
- Displacement in $X1$ and $X2$ direction is zero at intersection of mid plane and $X3 = 0$ surface
- $\phi = 0$ at $X1 = H$ surface

The electrical potential has been applied on the surface $X1 = 0$ with the increment $\Delta\phi = 10^{-4}$. Fig.5.6 shows the actuated state of the bending actuator.Fig.5.7 shows the

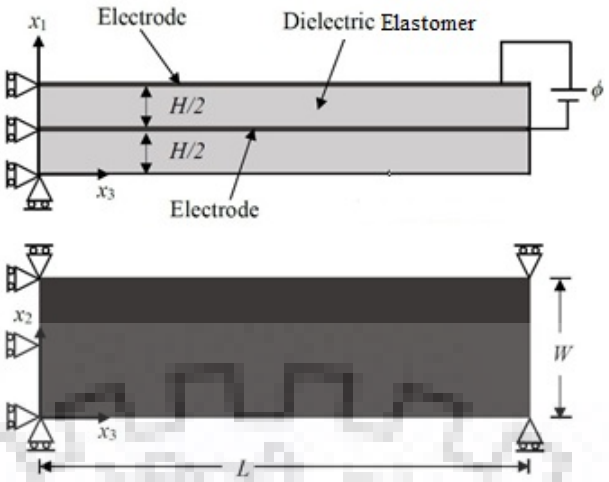

Figure 5.5: Geometry of the bi-layered bending actuator

relationship between tip displacement and the applied voltage.

5.3 Bursting Drop in DEA film

This example consider a bursting drop inside a DEA film. In this problem the electro-mechanical instability arises on the periphery of the droplet of the conductive fluid inserted within the DE. This problem have been studied experimentally[Wang et al., 2012]. This bubble will elongate in the crack like fashion towards the edges where voltage is applied. Due to the symmetry in the problem we have consider a quarter part of the plate as shown in the Fig.The voltage is applied on the top surface of the film and the bottom surface and the inner periphery of the bubble is grounded. We can see that, as the voltage increases, the drop starts to take the ellipse shape. It evolves in a shape of fine crack. Fig.5.5 shows position of the tip of the major axis of the drop with respect to the applied electric field. This result is nearly identical to the one carried out in[Seifi and Park, 2016]. Conductive fluid droplet in the DE can cause failure well below the critical voltages required for the pull-in instability[Wang et al., 2012]. And as shown in the Fig.5.5, once the sharp edge has been generated, it propagates through the film vary rapidly. If we continue to apply electric field even after formation of sharp tip, it will travel rapidly and will not recover its shape on switching off electrical field after that point. Wang et al. have shown experimentally that this leads to the tube shape separation in the film.

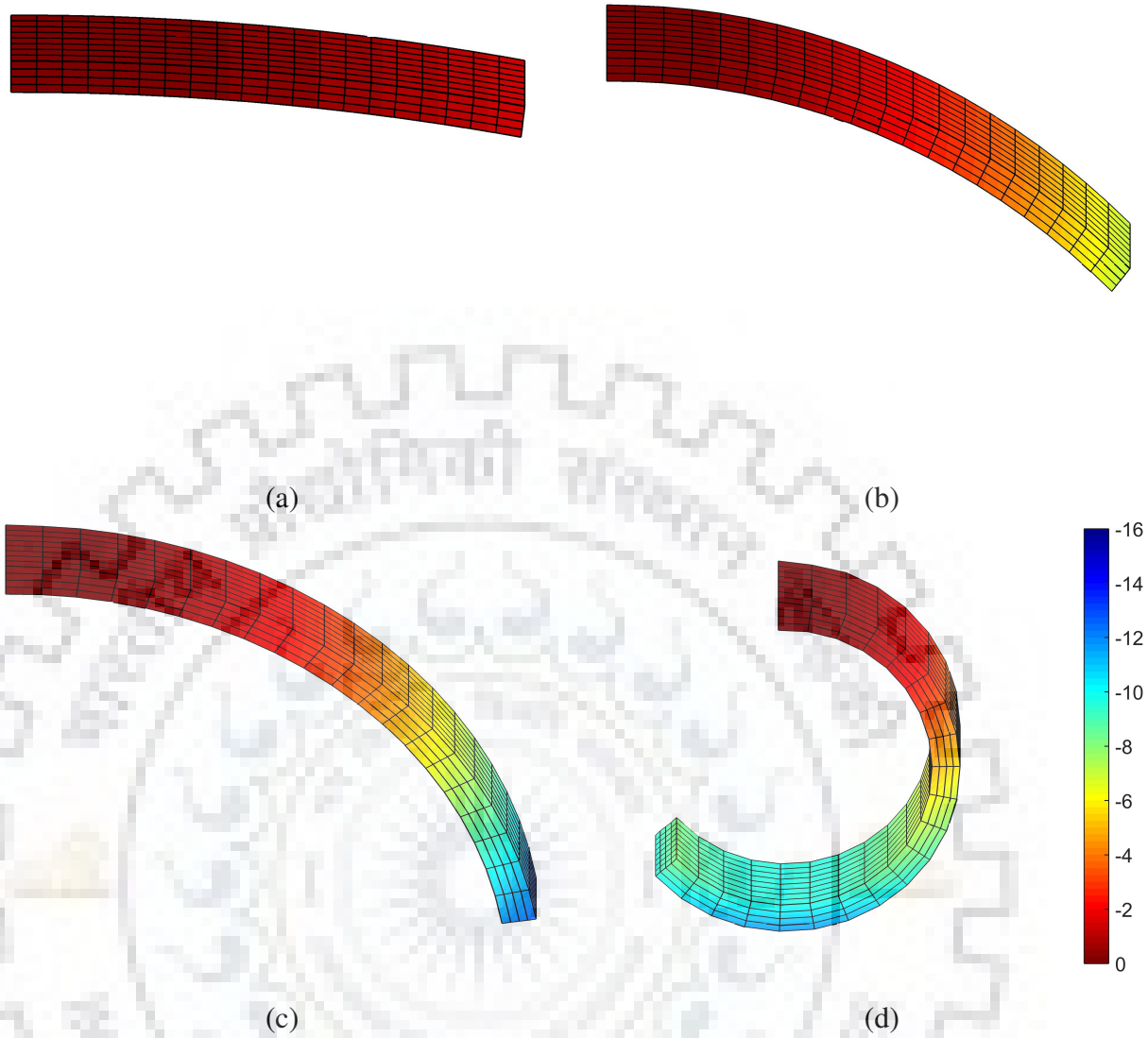

Figure 5.6: Deformation of the bending actuator on different level of electrical potential (a)$\phi = 0.08$ (b)$\phi = 0.15$ (c)$\phi = 0.23$ (d)$\phi = 0.35$

5.4 Computational Efficiency and Accuracy of the staggered formulation

In this section, we will discuss the computational efficiency and the accuracy of the staggered formulation in comparison with the monolithic formulation. We will consider the above discussed bubble drop problem for this. To provide a better condition for solution in both the formulations, we will use the normalized material parameters, i.e. $\mu = 1Pa$, $\varepsilon = 1F/m$ and density $\rho = 1$. The geometry used for both the formulation is same as discussed in the previous section. And, both the formulations have been implemented using the in-house MATLAB®. code for one to one compaision.

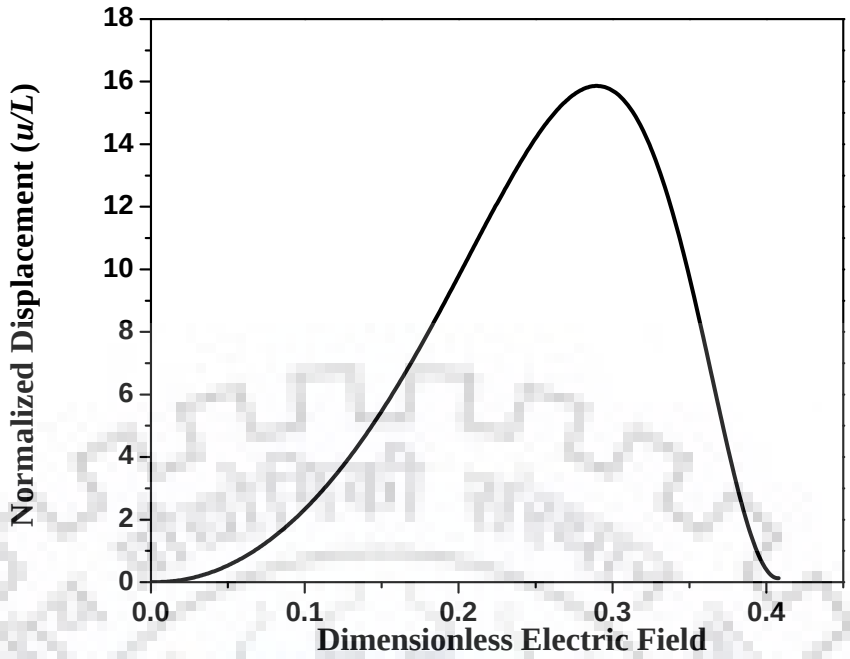

Figure 5.7: Response of the bending actuator normalized tip displacement (u_1/L) versus dimensionless electric field

Fig.5.5 shows the normalized tip displacement of the bubble drop with respect to electrical potential applied. The plot compares the results from staggered and monolithic formulations. From this plot, it is evident that predictions from both the formulations are in close agreement with each other. This shows the accuracy of the staggered formulation. Now, the same problem has been solved using the different mesh grid sizes of 21×21, 41×41 and 61×61. Fig.5.6 shows the ratio of time taken by the staggered formulation(t_s) to that by the monolithic formulation(t_m) for different mesh sizes. Apparently, staggered formulation takes less time for the solution and also, as the mesh size increases, time taken by the staggered formulation decreases significantly with respect to the monolithic formulation.

5.5 Wrinkling instability in DEA film

As discussed in the chapter 1, DE are thin membranes undergoing large deformations and they provide negligible resistance against bending. So, a small amount of compressive stress produced in the film will result in buckling in the out of plane direction. This will cause the surface of the actuator to deteriorate and it can not perform the intended function. In the Fig.5.7, a 2D dielectric elastomer, under plane strain

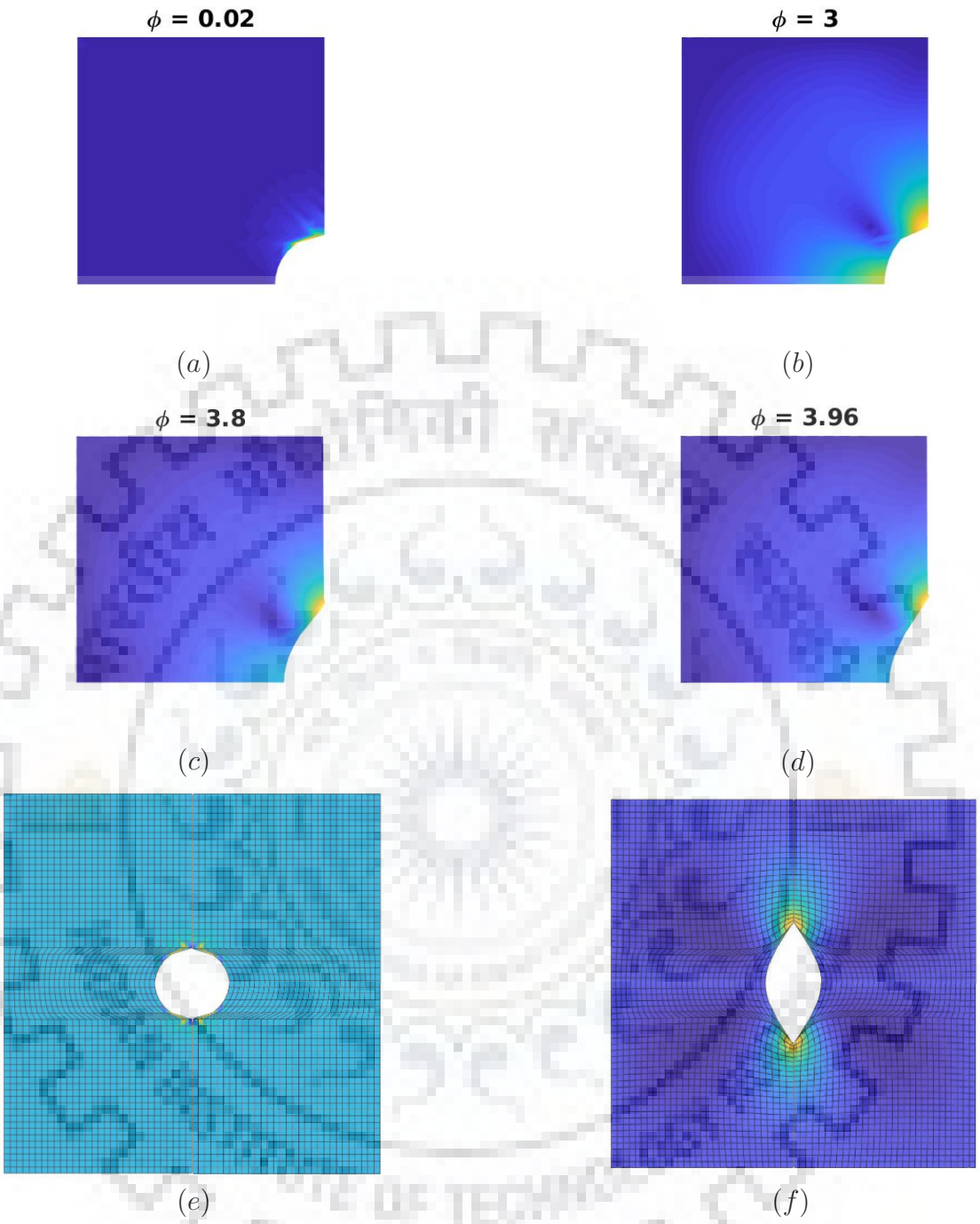

Figure 5.4: Deformation of the bubble drop for different level of electrical potential

condition has been shown. It is $1 \times 10mm$ film with roller supports on the both lateral side which prevents the lengthwise deformation. It has been fixed on the bottom side with the grounded base and the voltage is supplied on the upper side of the film. Fig.5.8 shows the deformation of the corner node with respect to the nominal dimensionless electric field applied. Fig.5.7 also shows the deformation at different level of voltage applied. As we can see, the wrinkling will start from the constrained boundaries and will

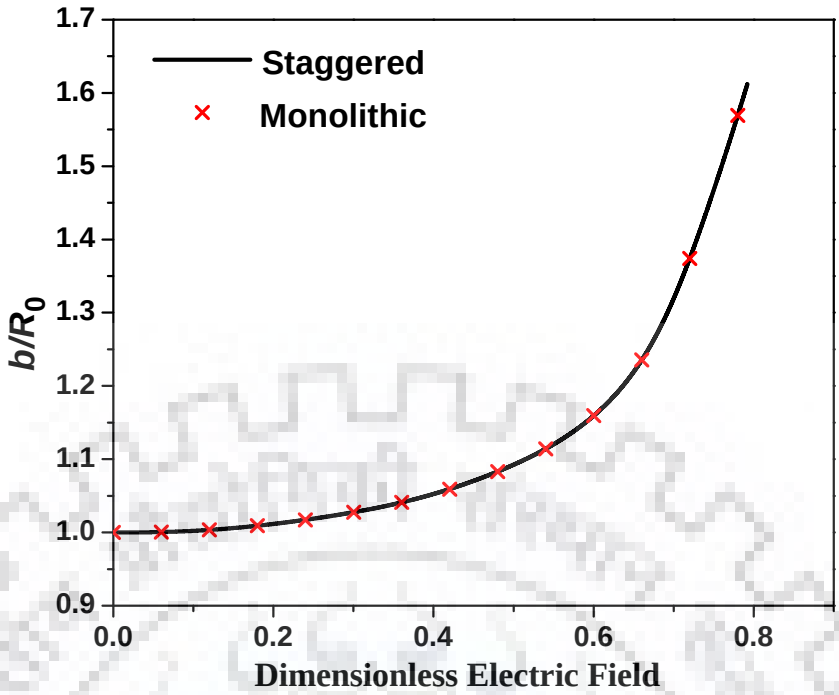

Figure 5.5: Position of the bursting drop tip b/R_0 with respect to nominal dimensionless electric field, where R_0 is the starting radius of the drop, and b is the long axis

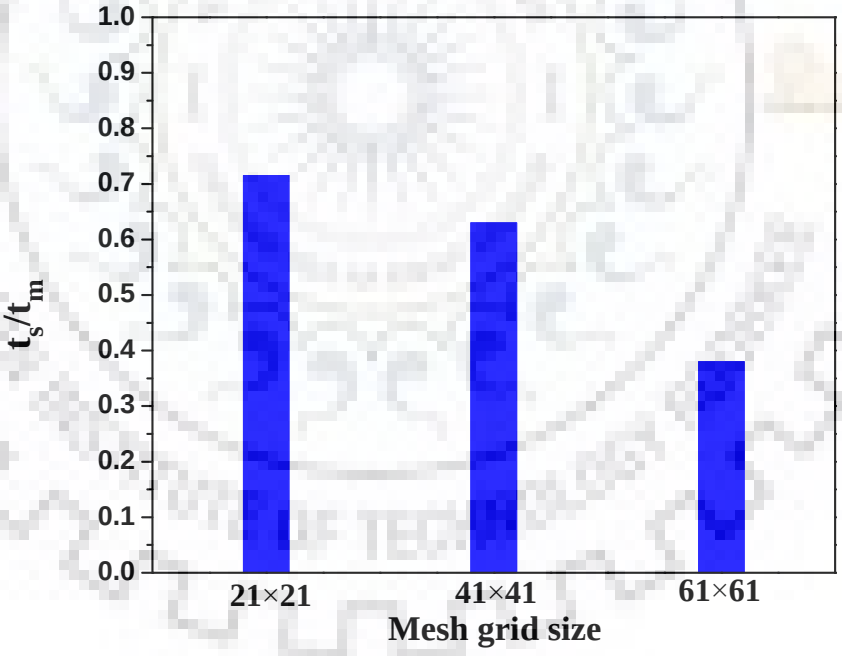

Figure 5.6: Ratio of the computation time taken by the staggered formulation to that by the monolithic formulation for different mesh density

propagate through the remaining portion of the film. Because of the boundary conditions, wrinkling is seen in the DE film before the pull-in failure of the film and can be taken as the warning call before the catastrophic failure of the system. But, this code was not able to perfectly capture the wrinkling pattern after the instability. Seifi and Park

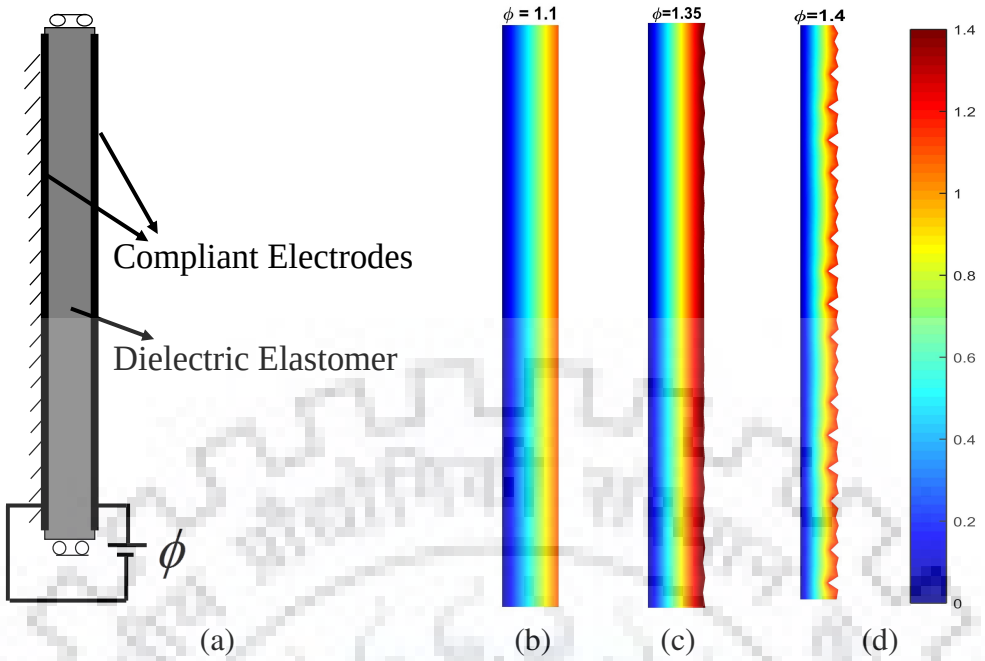

Figure 5.7: (a)Boundary conditions for the wrinkling problem and deformation of the elastomer at different level of electric potential (b)$\phi = 1.1$ (c)$\phi = 1.35$ (d)$\phi = 1.4$

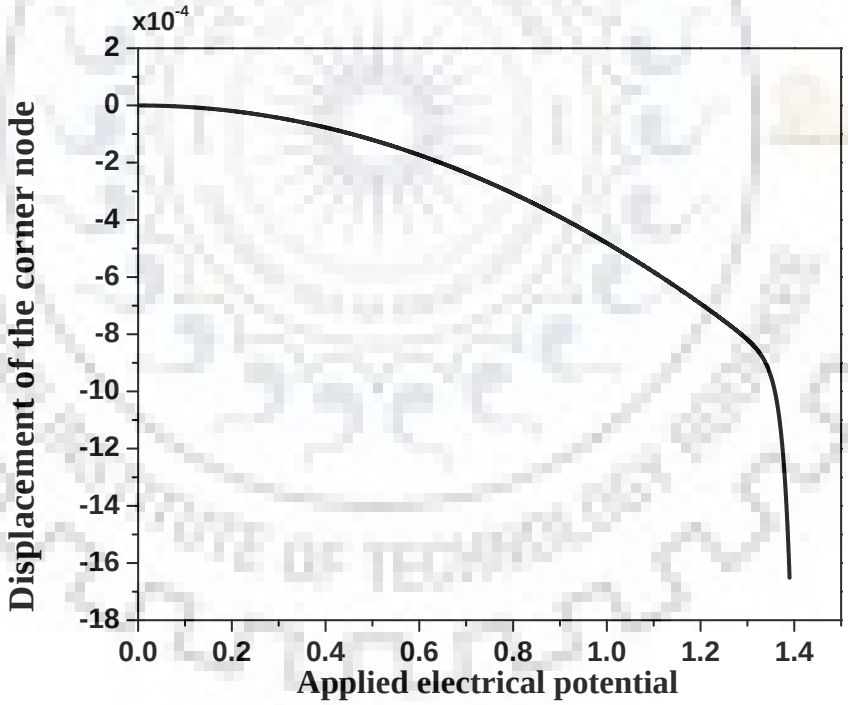

Figure 5.8: Electrical potential-Displacement for the dielectric film

[Seifi and Park, 2016] has shown that inclusion of elasto-capillary phenomena in the energy based approach can help to capture the surface instabilities more accurately.

Chapter 6

Conclusion

Summary

As soft smart materials, Dielectric elastomers have potential to be used in many fields and to utilize it in different field applications, it is important to study its response under different electro-mechanical loading conditions. The present work gives a non-linear finite element formulation for the Dielectric elastomers, which also accommodates the inertial effects. An in-house MATLAB®. code has been developed to simulate this formulation. It utilizes the $Q1P0$ elements to alleviate the problem of volumetric locking in the elastomer. The dynamic formulation for the same is based on the staggered solution technique. We have used Neo-Hookean model to simulate the hyperelastic response of the elastomer and ideal dielectric model to simulate the electro-mechanical coupling of the system.

Both static and dynamic formulations are validated with the instability parameters of the dielectric elasomers available in the literature. Voltage-stretch curves for static and dynamic cases have been obtained numerically and compared with the analytical results. Effect of the pre-stretch has also been studied for the static actuation. It can be observed that the static instability parameters value increases with increase in pre-stretch and higher level of actuation can be obtained. Some actuators with the complex loading conditions like bending and buckling actuators have also been studied. The developed code was able to simulate the response very well.

The problem of bursting conductive drop and wrinkle are also simulated and studied. Accuracy and the computational efficiency of the staggered formulation is compared

with the monolithic approach for the bursting drop problem. The resulats from both the approaches strongly agree with each other. And, we can evidently say that staggered approach is computationally efficient with respect to monolithic one and it becomes more efficient as the grid size of the problem increases. These results show the robustness of the developed method to handle different loading conditions and instabilities in the dielectric elastomer. But, some further improvement can be carried out in the formulation to tackle some more complex conditions.

Future Scope

- The Neo-Hookean material model has been used for all the simulations in the report. But, some more complex material models like Mooney-Rivlin model, Ogden Model, Gent model can be used in the same formulation for more accurately simulating hyperelastic behavior of the elastomer.
- This code was not able to accurately capture the profile of the elastomer after it wrinkles. So, the elasto-capillary effect can be incorporated in the same code for that.
- We have consider the isotropic elastomer material for the analysis. It can be extended for the anisotropic and viscoelastic materials by updating the energy density function.

Bibliography

[Bar-Cohen et al., 2007] Bar-Cohen, Y., Kim, K. J., Choi, H. R., and Madden, J. D. (2007). Electroactive polymer materials. *Smart Materials and Structures*, 16(2).

[Bar-Cohen et al., 1999] Bar-Cohen, Y., Leary, S. P., Shahinpoor, M., Harrison, J. S., and Smith, J. G. (1999). Flexible low-mass devices and mechanisms actuated by electroactive polymers. In *Smart Structures and Materials 1999: Electroactive Polymer Actuators and Devices*, volume 3669, pages 51–57. International Society for Optics and Photonics.

[Brochu and Pei, 2010] Brochu, P. and Pei, Q. (2010). Advances in dielectric elastomers for actuators and artificial muscles. *Macromolecular rapid communications*, 31(1):10–36.

[Carpi, 2010] Carpi, F. (2010). Electromechanically active polymers. *Polymer International*, 59(3):277–278.

[Carpi et al., 2003] Carpi, F., Chiarelli, P., Mazzoldi, A., and De Rossi, D. (2003). Electromechanical characterisation of dielectric elastomer planar actuators: comparative evaluation of different electrode materials and different counterloads. *Sensors and Actuators A: Physical*, 107(1):85–95.

[Gatti et al., 2014] Gatti, D., Haus, H., Matysek, M., Frohnapfel, B., Tropea, C., and Schlaak, H. F. (2014). The dielectric breakdown limit of silicone dielectric elastomer actuators. *Applied Physics Letters*, 104(5):052905.

[Giousouf and Kovacs, 2013] Giousouf, M. and Kovacs, G. (2013). Dielectric elastomer actuators used for pneumatic valve technology. *Smart Materials and Structures*, 22(10):104010.

[Goulbourne et al., 2005] Goulbourne, N., Mockensturm, E., and Frecker, M. (2005). A nonlinear model for dielectric elastomer membranes. *Journal of Applied Mechanics*, 72(6):899–906.

[Hong, 2011] Hong, W. (2011). Modeling viscoelastic dielectrics. *Journal of the Mechanics and Physics of Solids*, 59(3):637–650.

[Hughes, 2012] Hughes, T. J. (2012). *The finite element method: linear static and dynamic finite element analysis*. Courier Corporation.

[Joglekar, 2014] Joglekar, M. (2014). An energy-based approach to extract the dynamic instability parameters of dielectric elastomer actuators. *Journal of Applied Mechanics*, 81(9):091010.

[Joglekar, 2015] Joglekar, M. (2015). Dynamic-instability parameters of dielectric elastomer actuators with equal biaxial prestress. *AIAA Journal*, 53(10):3129–3133.

[Li et al., 2018] Li, K., Wu, W., Jiang, Z., and Cai, S. (2018). Voltage-induced wrinkling in a constrained annular dielectric elastomer film. *Journal of Applied Mechanics*, 85(1):011007.

[Li et al., 2013] Li, T., Keplinger, C., Baumgartner, R., Bauer, S., Yang, W., and Suo, Z. (2013). Giant voltage-induced deformation in dielectric elastomers near the verge of snap-through instability. *Journal of the Mechanics and Physics of Solids*, 61(2):611–628.

[Liu et al., 2017] Liu, J., Foo, C. C., and Zhang, Z.-Q. (2017). A 3d multi-field element for simulating the electromechanical coupling behavior of dielectric elastomers. *Acta Mechanica Solida Sinica*, 30(4):374–389.

[Mao et al., 2015] Mao, G., Huang, X., Diab, M., Li, T., Qu, S., and Yang, W. (2015). Nucleation and propagation of voltage-driven wrinkles in an inflated dielectric elastomer balloon. *Soft Matter*, 11(33):6569–6575.

[Nam and Kwan, 2012] Nam, D. N. C. and Kwan, A. K. (2012). Ionic polymer metal composite transducer and self-sensing ability. In *Smart Actuation and Sensing Systems-Recent Advances and Future Challenges*. IntechOpen.

[O'Brien et al., 2009] O'Brien, B., McKay, T., Calius, E., Xie, S., and Anderson, I. (2009). Finite element modelling of dielectric elastomer minimum energy structures. *Applied Physics A*, 94(3):507–514.

[O'Halloran et al., 2008] O'Halloran, A., O'malley, F., and McHugh, P. (2008). A review on dielectric elastomer actuators, technology, applications, and challenges. *Journal of Applied Physics*, 104(7):9.

[Park et al., 2012] Park, H. S., Suo, Z., Zhou, J., and Klein, P. A. (2012). A dynamic finite element method for inhomogeneous deformation and electromechanical instability of dielectric elastomer transducers. *International Journal of Solids and Structures*, 49(15-16):2187–2194.

[Pelrine et al., 2000a] Pelrine, R., Kornbluh, R., Joseph, J., Heydt, R., Pei, Q., and Chiba, S. (2000a). High-field deformation of elastomeric dielectrics for actuators. *Materials Science and Engineering: C*, 11(2):89–100.

[Pelrine et al., 2000b] Pelrine, R., Kornbluh, R., Pei, Q., and Joseph, J. (2000b). High-speed electrically actuated elastomers with strain greater than 100%. *Science*, 287(5454):836–839.

[Pelrine et al., 2001] Pelrine, R., Kornbluh, R. D., Eckerle, J., Jeuck, P., Oh, S., Pei, Q., and Stanford, S. (2001). Dielectric elastomers: generator mode fundamentals and applications. In *Smart Structures and Materials 2001: Electroactive Polymer Actuators and Devices*, volume 4329, pages 148–157. International Society for Optics and Photonics.

[Pelrine et al., 1998] Pelrine, R. E., Kornbluh, R. D., and Joseph, J. P. (1998). Electrostriction of polymer dielectrics with compliant electrodes as a means of actuation. *Sensors and Actuators A: Physical*, 64(1):77–85.

[Plante and Dubowsky, 2006] Plante, J.-S. and Dubowsky, S. (2006). Large-scale failure modes of dielectric elastomer actuators. *International journal of solids and structures*, 43(25-26):7727–7751.

[Qu and Suo, 2012] Qu, S. and Suo, Z. (2012). A finite element method for dielectric elastomer transducers. *Acta Mechanica Solida Sinica*, 25(5):459–466.

[Roddeman et al., 1987] Roddeman, D., Drukker, J., Oomens, C., and Janssen, J. (1987). The wrinkling of thin membranes: Part i—theory. *Journal of Applied Mechanics*, 54(4):884–887.

[Seifi and Park, 2016] Seifi, S. and Park, H. S. (2016). Computational modeling of electro-elasto-capillary phenomena in dielectric elastomers. *International Journal of Solids and Structures*, 87:236–244.

[Shankar et al., 2007] Shankar, R., Ghosh, T. K., and Spontak, R. J. (2007). Dielectric elastomers as next-generation polymeric actuators. *Soft Matter*, 3(9):1116–1129.

[Sharma et al., 2017] Sharma, A. K., Bajpayee, S., Joglekar, D., and Joglekar, M. (2017). Dynamic instability of dielectric elastomer actuators subjected to unequal biaxial prestress. *Smart Materials and Structures*, 26(11):115019.

[Suo et al., 2008] Suo, Z., Zhao, X., and Greene, W. H. (2008). A nonlinear field theory of deformable dielectrics. *Journal of the Mechanics and Physics of Solids*, 56(2):467–486.

[Tröls et al., 2013] Tröls, A., Kogler, A., Baumgartner, R., Kaltseis, R., Keplinger, C., Schwödiauer, R., Graz, I., and Bauer, S. (2013). Stretch dependence of the electrical breakdown strength and dielectric constant of dielectric elastomers. *Smart Materials and Structures*, 22(10):104012.

[Vossen et al., 2008] Vossen, B., Joni, H. J., and Peerlings, R. (2008). Volumetric locking in finite elements. *Bachelor Thesis, Eindhoven University of Technology, Eindhoven, The Netherlands*.

[Wang et al., 2012] Wang, Q., Suo, Z., and Zhao, X. (2012). Bursting drops in solid dielectrics caused by high voltages. *Nature communications*, 3:1157.

[Wissler and Mazza, 2007] Wissler, M. and Mazza, E. (2007). Mechanical behavior of an acrylic elastomer used in dielectric elastomer actuators. *Sensors and Actuators A: Physical*, 134(2):494–504.

[Zhao and Sharma, 2017] Zhao, X. and Sharma, P. (2017). Avoiding the pull-in instability of a dielectric elastomer film and the potential for increased actuation and energy harvesting. *Soft Matter*, 13(26):4552–4558.

[Zheng, 2009] Zheng, L. (2009). *Wrinkling of dielectric elastomer membranes*. California Institute of Technology.

[Zhou et al., 2008] Zhou, J., Hong, W., Zhao, X., Zhang, Z., and Suo, Z. (2008). Propagation of instability in dielectric elastomers. *International Journal of Solids and Structures*, 45(13):3739–3750.